Small Structures

WILEY VCH

small structures

REVIEW OPEN ACCESS

Micropatterned Surfaces with Unidirectional Wetting Properties for Liquid Transport

Elham Lori Zoudani[1] | Prabuddha De Saram[1] | Stefanie Feih[2,3] | Hoang Huy Vu[1] | Nam-Trung Nguyen[1] | Navid Kashaninejad[1,2]

[1]Queensland Quantum and Advanced Technologies Research Institute, Griffith University, Nathan, Australia | [2]School of Engineering and Built Environment, Griffith University, Nathan, Australia | [3]Advanced Design and Prototyping Technologies (ADaPT) Institute, Griffith University, Gold Coast, Australia

Correspondence: Nam-Trung Nguyen (nam-trung.nguyen@griffith.edu.au) | Navid Kashaninejad (n.kashaninejad@griffith.edu.au)

Received: 24 July 2025 | **Revised:** 9 October 2025 | **Accepted:** 10 October 2025

Funding: Australian Research Council (ARC), Discovery Early Career Research Award (DECRA), Grant/Award Number: DE220100205; Australian Research Council (ARC), Australian Laureate Fellowship, Grant/Award Number: FL230100023

Keywords: anisotropic wetting surfaces | droplet manipulation | micropatterned surfaces | unidirectional wetting

ABSTRACT

Interest in micropatterned surfaces with unidirectional wetting properties has grown significantly due to their unique ability to enable controlled liquid manipulation. This property is essential for diverse applications, including microfluidics, water harvesting, and self-cleaning systems, where directional droplet motion promotes efficient removal of contaminants and reduces surface fouling. Despite extensive research on anisotropic wetting, a comprehensive framework encompassing design considerations, fabrication methods, and practical challenges for unidirectional liquid transport remains underdeveloped. This review paper addresses this gap by presenting a holistic overview of micropatterned anisotropic surfaces and their wetting behaviors in unidirectional fluid handling. Key mechanisms of liquid transport, ranging from passive modes such as gravity and wettability gradient to active modes involving external stimuli, are discussed. This review critically evaluates surface fabrication techniques, highlighting their advantages and limitations. By critically analyzing recent advances and identifying key structure–function relationships, this review offers design principles and emerging fabrication strategies that can accelerate the development of next-generation micropatterned surfaces for directional liquid transport in microfluidics, diagnostics, and surface engineering.

1 | Introduction

Surface wetting, defined as the interaction between a liquid and a solid surface, is a function of both chemical composition and physical morphology of the surface [1]. Wetting is typically characterized by the contact angle generated by a water droplet on a surface. Surfaces with water contact angles less than 90° are categorized as hydrophilic, while those with contact angles greater than 90° are hydrophobic. Another crucial parameter in wetting is the sliding angle, which quantifies the stability of a droplet. The sliding angle is defined as the inclination at which a droplet begins to slide on the slope [2]. Surfaces with a contact angle greater than 150° and a sliding angle less than 10° are referred to as superhydrophobic and are highly effective in repelling liquids [3, 4].

A surface exhibits isotropic wettability if a liquid droplet has the same contact angle in all directions [5]. In contrast, anisotropic wetting occurs when liquid distribution along the contact line varies depending on the direction [6], leading to directional liquid droplet spreading in wetting states and controlled movement in nonwetting [5, 6]. Unlike isotropic surfaces, where liquid moves randomly, anisotropic surfaces guide it in predetermined directions. Anisotropic wetting arises from either asymmetrical

This is an open access article under the terms of the Creative Commons Attribution License, which permits use, distribution and reproduction in any medium, provided the original work is properly cited.

© 2025 The Author(s). *Small Structures* published by Wiley-VCH GmbH.

surface morphology or chemical heterogeneity [7–9]. Structures such as micropillars, grooves, or chemical gradients induce macroscopic changes in droplet behavior, enabling precise control of liquid motion [5, 10].

Controlled liquid transport, particularly through surface wettability manipulation, enables efficient handling of small liquid volumes [11]. Directional wetting is highly advantageous for controlled liquid manipulation in fields such as microfluidics [12, 13], water collection [14], and anti-adhesion surfaces, where such liquid motion helps prevent the accumulation of contaminants or biofouling agents [15, 16]. These surface innovations are also driving progress in areas such as biosensing and energy systems.

The initial design concept for these types of surfaces can originate from either biological organisms or theoretical principles aimed at achieving unidirectional wettability. Nature offers elegant solutions, such as the hierarchical structures on rice leaves or the legs of water striders, which enable droplet motion without the need for external power [7, 17]. Engineers replicate these principles or develop tailored designs using wettability gradients, unique surface patterns, or stimuli-responsive materials [18, 19].

Liquid motion on these surfaces can occur either passively, e.g., via gravity and surface features or actively, using external triggers like light, heat, or electric fields [20, 21]. The chosen strategy directly influences the overall morphological and surface design considerations.

Despite significant advancements, existing studies on anisotropic surfaces primarily focus on isolated designs or specific applications. A recent review highlights bioinspired surfaces for interfacial liquid manipulation and their innovative applications [22]. Our presented review, in contrast, emphasizes micropatterned anisotropic wetting surfaces specifically designed for unidirectional liquid transport. It furthermore in-depth examines the interplay between morphological factors, material properties, and their integration with physical characteristics to achieve targeted anisotropic surface wettability. Particular attention is given

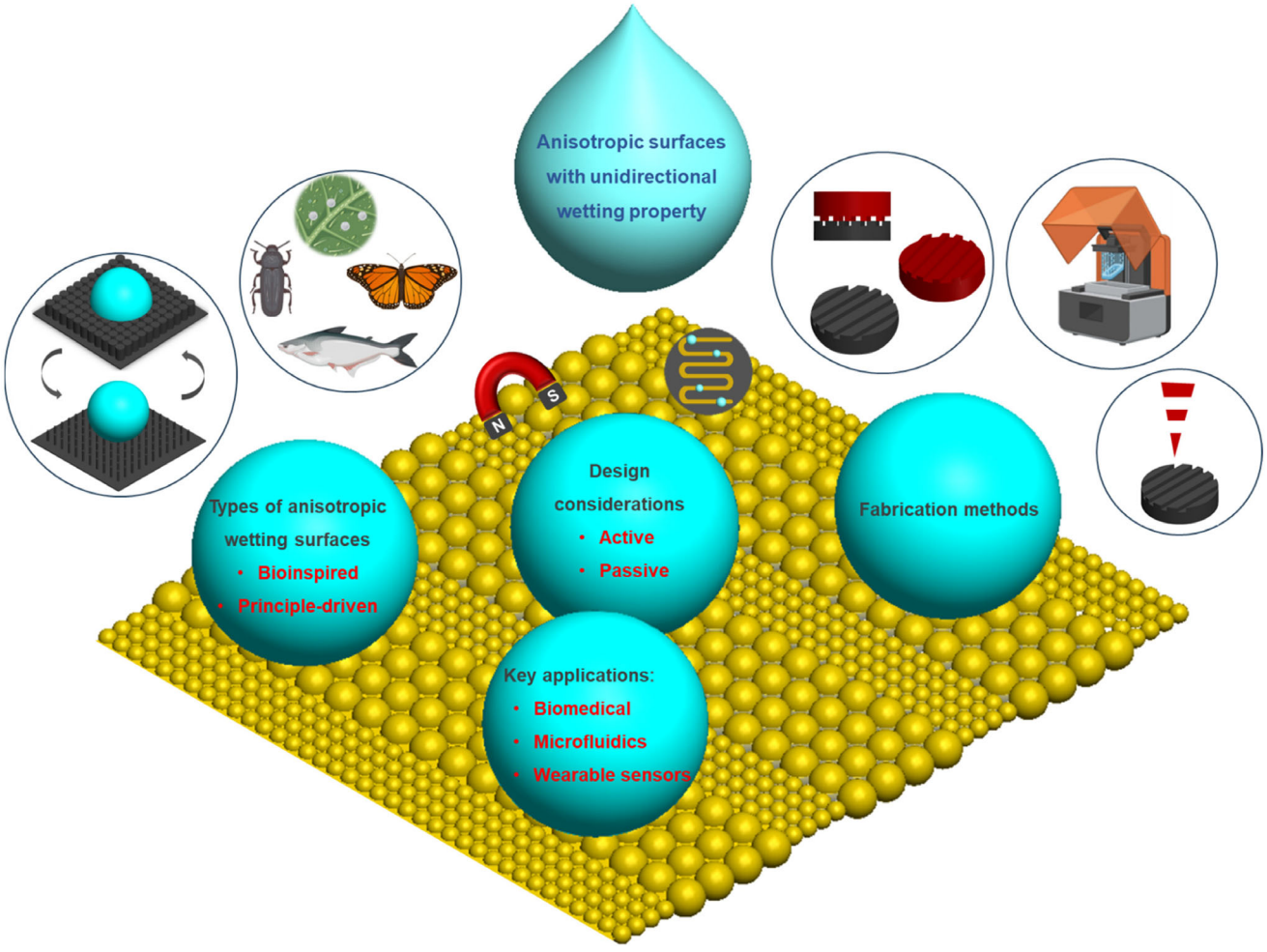


FIGURE 1 | Overview of key topics covered in this review on micropatterned anisotropic surfaces with unidirectional wetting properties. The diagram highlights four major themes: (i) key applications in biomedical devices, microfluidics, and wearable sensors; (ii) types of anisotropic wetting surfaces (bioinspired and principle-driven); (iii) fabrication methods, including laser micromachining and 3D printing; and (iv) design considerations, categorized into active and passive mechanisms. Insets include representative examples from nature (e.g., beetle, butterfly, fish, and plant leaves) and schematic illustrations of fabrication strategies such as laser machining and 3D printing. Insets of the biocreatures and the printing machine are created in BioRender. https://BioRender.com/ y07z351.

26884062, 2026, 2, Downloaded from https://onlinelibrary.wiley.com/doi/10.1002/sstr.202500492 by Scholarly Resource Services, Wiley Online Library on [04/11/2026]. See the Terms and Conditions (https://onlinelibrary.wiley.com/terms-and-conditions) on Wiley Online Library for rules of use; OA articles are governed by the applicable Creative Commons License

to how selecting specific micropatterns influences subsequent preparation steps.

Figure 1 outlines the core themes addressed in this review, filling the critical gap in the literature by systematically connecting application-driven demands with the design and fabrication of micropatterned anisotropic surfaces. As the need for directional liquid handling continues to grow in emerging technologies, ranging from biomedical diagnostics to water harvesting, there is a clear demand for surfaces with tailored unidirectional wetting behaviors. The building blocks of this review are organized to provide a comprehensive and logical progression from motivation to implementation. Following the introduction, we first provide an overview of the different types of micropatterned anisotropic surfaces, including both bioinspired and principle-driven designs. We then present key design considerations that influence the behavior and performance of liquids to support next-generation liquid transport solutions. This is followed by a detailed discussion of fabrication methods, categorized by the type of anisotropy (geometrical or chemical), which serves as the foundational framework for designing and fabricating such surfaces. The review then examines current and emerging applications of unidirectional wetting surfaces to highlight their practical relevance, before concluding with a discussion of existing challenges and future research directions.

It should be noted that while this review addresses both droplet-based and bulk liquid movement, the primary focus is on droplet transport. This focus provides a more direct and widely applicable framework for studying and designing micropatterned surfaces with unidirectional wetting properties.

2 | Anisotropic Surfaces with Unidirectional Wetting Properties

We have categorized the anisotropic surfaces based on their underlying design origins into two categories: bioinspired and principle-driven. This classification reflects the source of conceptual inspiration. Bioinspired anisotropic surfaces are derived from observations of biological systems or natural organisms, where morphological or functional features are mimicked and engineered to achieve similar wetting behavior. Principle-driven anisotropic surfaces are designed and fabricated based on fundamental physical, chemical, or material science principles.

2.1 | Bioinspired Anisotropic Surfaces

Nature has always served as a fundamental reference for the design and development of structures across various scientific disciplines [23–25]. Over millions of years, biological systems have evolved micro- and nanoscale surface features that enhance wetting properties [26]. Extensive research has been dedicated to understanding these natural structures, particularly in those exhibiting directional wetting behavior. Biologically anisotropic wetting surfaces in plants and animals demonstrate the ability to transport water droplets unidirectionally [27–30]. This directional liquid movement often serves critical functions, such as enhancing water collection efficiency, reducing surface contamination, or minimizing added weight, all of which contribute to the organism's survival and energy efficiency. These natural surfaces typically feature hierarchically organized micro/nanostructures and/or spatially varying material wettabilities, which together guide liquid motion along preferred paths.

For instance, rice leaves display anisotropic droplet rolling behavior due to their surface microgrooves [28]. Water droplets can move only along directions parallel to the leaf edges, while their perpendicular movement is restricted. Similarly, bamboo leaves exhibit anisotropic wetting behavior, evident from the elliptical shape of water droplets on their surfaces caused by the alignment of leaf veins [31]. On butterfly wings, Zheng et al. [32] demonstrated that water droplets move outward radially along specific patterns but are pinned when rolling in the opposite direction.

Inspired by natural systems, researchers have designed and developed biomimetic anisotropic surfaces to control liquid behavior in a direction-selective manner. For example, Cao et al. [33] created a smart fluid-controlled surface combining the unidirectional wettability of butterfly wings, the slippery surface of pitcher plants, and the motile microcilia of microorganisms. This surface, featuring magneto-responsive microstructures, facilitated continuous directional droplet adhesion and sliding.

Similarly, Song et al. [34] utilized a cross-species bionic design approach to develop an anisotropic wetting surface with an array of micropillars for active, unidirectional droplet transport. Inspired by the anisotropic wettability of rice leaves and the directional movement of motile microcilia, the design incorporated a high-aspect-ratio magnetically responsive microcolumn array (HAR-MRMA). This system allowed droplets to be directionally transported by an external magnetic field, enabling multifunctional droplet motion, including straight-line, circular, and parallel movements. Notably, the HAR-MRMA structure allowed horizontal droplet movement on inclined surfaces, overcoming the limitations of other cilia-like structures.

Zhang et al. [35] developed an anisotropic slippery cilia surface (ASCS) combining the flexible asymmetric microstructures of butterfly wings (*Morpho aega*) and the slippery properties of pitcher plants (*Nepenthes alata*). By adjusting the elastic modulus of the surface, they achieved asymmetric bubble transport. In low elastic modulus conditions (soft cilia), bubbles moved toward the cilia tilt direction, whereas with high elastic modulus (hard cilia), they moved against it. This behavior was attributed to differing three-phase contact line (TCL) asymmetries and resistance forces. The ASCS, doped with magneto-responsive cobalt particles, allowed for real-time, switchable bubble transport by externally modulating the cilia's structural properties.

Using materials with unique properties to mimic the functional behaviors of natural organisms has brought artificial surfaces closer to their biological counterparts. For example, Wang et al. [36] designed a superhydrophobic surface with shape-memory adhesion inspired by the back-scrolling/unfolding ability of gecko toe pads (see Figure 2A). The structure, comprising hair-like pillars with a superhydrophobic layer, was integrated with a shape-memory polyurethane-cellulose nanofiber (PU-CNF) substrate to simulate gecko muscle behavior. This system enabled the

26884062, 2026, 2, Downloaded from https://onlinelibrary.wiley.com/doi/10.1002/sstr.202500492 by Scholarly Resource Services, Wiley Online Library on [04/11/2026]. See the Terms and Conditions (https://onlinelibrary.wiley.com/terms-and-conditions) on Wiley Online Library for rules of use; OA articles are governed by the applicable Creative Commons License

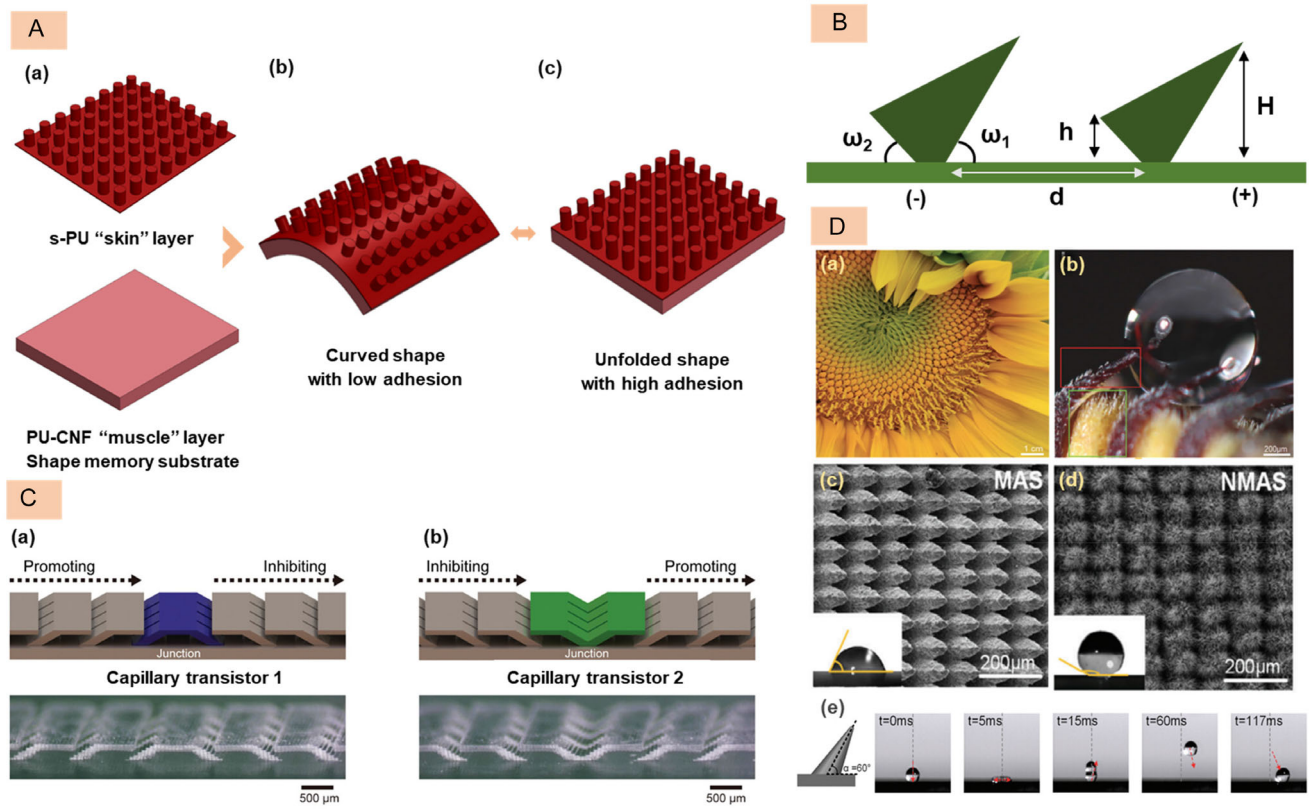


FIGURE 2 | Examples of the bioinspired micropatterned surfaces with unidirectional wetting property. (A) Schematic illustration of the preparation mechanism of the gecko toe pads inspired superhydrophobic shape memory film. (a) A superhydrophobic layer consisting of an array of pillar structures, resembling hair-like gecko toe pads, was stuck onto a shape memory polyurethane-cellulose nanofiber (PU-CNF) substrate to simulate the muscle of gecko toe pads. (b), (c) Through deforming the structure, reversible surface/droplet adhesion states (low and high) were generated. Modified from Ref. [36], Copyright 2019, Royal Society of Chemistry (RSC). (B) Schematic of CMIA. Structural characteristics: upper height (H), lower height (h), bottom-to-bottom spacing (d), upper tilting re-entrant angle (ω_1), and lower tilting re-entrant angle (ω_2). The positive (+) and negative (−) signs indicate the direction of liquid movement. Modified from Ref. [37], Copyright 2024, American Association for the Advancement of Science (AAAS). (C) (a) Schematic (top) and optical image (bottom) of the capillary transistor with re-entrant structures tilting toward the center, where the left side promotes the liquid transport and the right side inhibits the flow. (b) Schematic (top) and optical image (bottom) of the capillary transistor with re-entrant structures tilting opposite the center, the left side inhibits the fluid flow, and the right side promotes the flow. Reprinted with permission from [38], Copyright 2024, Wiley-VCH (D) Schematic illustration of sunflower-inspired surfaces. (a) Optical picture of the sunflower. (b) State of the droplet sitting on the core of the sunflower. (c) SEM image of the morphology of nanosecond laser-fabricated microcone array surface (MAS) and droplet contact angle. (d) SEM image of the morphology of nanoneedle-modified microcone array surface (NMAS) and droplet state on the structure. (e) Bouncing performance of droplet on the microcone structures with an inclination angle of 60°. Reprinted with permission from [39], Copyright 2024, Wiley-VCH.

surface to memorize and repeatedly display different shapes and contact modes.

Inspired by *Crassula muscosa*, two sets of *C. muscosa*-inspired arrays (CMIAs) were fabricated for directional liquid transport [37]. Referring to the re-entrant structures of this plant, two modes of unidirectional liquid transport were observed, corresponding to the different leaf morphologies of the plant shoots. The key distinction lies in the tilting angles of the re-entrant structures. CMIA I and CMIA II mimic the re-entrant leaves but with different tilting re-entrant angles. Specifically, CMIA I has re-entrant angles of $\omega_1 = 70°$ and $\omega_2 = 40°$, while CMIA II has $\omega_1 = 51°$ and $\omega_2 = 57°$. Both types of CMIA share the same geometric dimensions, including the upper height (H, measured from the highest vertex to the base), the lower height (h, measured from the lower vertex to the bottom), and the interspacing distance, as illustrated in Figure 2B. Ethanol was chosen as the test liquid. On both CMIA types, ethanol exhibited the same wetting properties, with a static contact angle of 11.5° and an advancing angle of 21.5°. Despite these identical wetting behaviors, the two surfaces demonstrated selective unidirectional liquid transport. On CMIA I, ethanol moved unidirectionally in the negative direction and was pinned in the positive direction. In contrast, on CMIA II, the liquid flowed toward the positive direction and was blocked in the negative direction.

Owing to the analogies between fluid flow and electrical transport, several well-established concepts from electronics can be adapted to micropatterned platforms for directional liquid manipulation. By modifying design features, the concept of a capillary transistor was envisioned through the structural patterning of 3D re-entrant elements [38]. In electronics, a transistor is a semiconductor device used for amplifying or switching electrical currents. Similarly, bioinspired 3D-printed re-entrant structures with long overhangs and interconnected forward/lateral microchannels have been proposed to enhance vertical capillary

26884062, 2026, 2, Downloaded from https://onlinelibrary.wiley.com/doi/10.1002/sstr.202500492 by Scholarly Resource Services, Wiley Online Library on [04/11/2026]. See the Terms and Conditions (https://onlinelibrary.wiley.com/terms-and-conditions) on Wiley Online Library for rules of use; OA articles are governed by the applicable Creative Commons License

flow [38], see Figure 2C. Moreover, by introducing symmetry or asymmetry into the bioinspired structural design, the device can function as an amplifier or as a switch/valve to systematically adjust capillary flow direction, width, and rate.

Recently, Yang et al. designed and fabricated a sunflower-inspired superhydrophobic surface for liquid and ice droplet manipulation [39]. Drawing inspiration from the microconical structures in the sunflower core, which facilitate droplet collection, the researchers developed a nanoneedle-modified microcone array surface (NMAS). This surface was fabricated using a combination of nanosecond laser engraving and electroforming, followed by fluorination. Figure 2D illustrates the schematic design of the structure. The fabricated surface exhibited superhydrophobic properties, with a measured water contact angle of 152°. Droplet-bouncing experiments were conducted to evaluate its performance. The general morphological characteristics of the microstructures, including element dimensions and inclination angles, were tuned by adjusting the laser spot parameters. These adjustments significantly influenced the droplet bouncing behavior, with the longest recorded bouncing distance in the X direction (−0.8 mm) observed for microcone structures with a 60° inclination angle. Based on the results, droplets on the fabricated surface demonstrated the ability to achieve various programmed bouncing behaviors, including gravity-defying hopping and directional transport. Additionally, the results highlighted the surface's property of delayed icing and anti-icing.

2.2 | Principle-Driven Anisotropic Surfaces

Biomimicry offers powerful design insights, but blindly copying natural surfaces risks introducing unpredictable behavior, manufacturing inefficiencies, and functionality conflicts. Careful abstraction of the *single intended function*—stripping away extraneous biological roles—is essential for successful, application-specific industrial use. The term "principle-driven" has been coined to describe a type of anisotropic wetting surface that, from both general surface characteristics and functional perspective, is fundamentally developed based on a mechanistic understanding of key principles in chemistry, physics, and materials science. For instance, tunable wettability for droplet manipulation can be achieved by leveraging the unique properties of liquid crystal polymers (LCPs), whose surface functionality is governed by precise control over phase transitions and molecular alignment.

Engineered anisotropic wetting surfaces with tunable and reversible wettability or adhesion properties have been extensively explored for droplet manipulation in various practical applications [40, 41]. These approaches typically involve triggering changes in chemical and/or morphological properties of the surfaces using external stimuli. For instance, a light-controlled adhesion-switching mechanism was developed using an array of azobenzene liquid crystal polymer (LCP) superhydrophobic films for rapid, precise, and noncontact droplet manipulation [42]. The azobenzene LCP was chosen due to its photoisomerization and liquid crystallinity properties. Upon UV irradiation, the azobenzene mesogens transition to the *cis* state, increasing water droplet adhesion (pinning state) due to enhanced surface polarity. Under visible light irradiation, the mesogens revert to the *trans-state*, reducing surface adhesion.

Okada et al. fabricated paraffin-coated titanate nanorods that transition from superhydrophobic to less hydrophobic as the temperature increases [43]. This behavior arises from roughness changes due to paraffin's thermal expansion, enabling directional droplet motion through localized heating (Figure 3A). Similarly, Wang et al. developed a thermo-responsive liquid crystal elastomer (LCE) surface featuring micropillar arrays that fully collapse upon heating, converting a hydrophobic, rough surface to a smooth, hydrophilic one [44], (Figure 3B). This approach enables full reversibility, overcoming limitations in prior systems where roughness changes were only partial. Magnetically responsive surfaces also demonstrate rapid and reversible control. Hou et al. embedded iron powder within a soft PDMS film, forming vertical microstructures under an applied magnetic field that reduced droplet adhesion by minimizing contact area [47]. Removal of the field restored the flat, high-adhesion state within milliseconds.

In contrast to these externally triggered strategies, chemically patterned surfaces can induce unidirectional motion passively through wettability gradients. For instance, Liu et al. created superhydrophobic surfaces with uncoated triangular hydrophilic regions [48]. The boundary angle between wetting regions generated asymmetric Laplace pressure, enabling droplets (8–50 μL) to climb a 4° incline against gravity.

Despite their simplicity, chemically patterned surfaces often suffer from droplet pinning, limiting mobility. This limitation can be overcome using lubricated chemically heterogeneous (LCHet) surfaces, where a thin oil film preferentially dewets from hydrophilic to hydrophobic areas, creating anisotropic slippery channels [49]. As demonstrated by Sharma et al., such surfaces enable smooth motion along parallel directions and stick-slip behavior across stripes, with movement controlled by adjusting hydrophobic area fractions (Figure 3C) [45].

Expanding this concept, Rao et al. developed a near-infrared (NIR)-responsive slippery surface (G/NPGS) by integrating a graphene-embedded PDMS substrate with silicone oil infusion [50]. Under NIR irradiation, silicone oil was locally released to the targeted surface areas, generating dynamic wettability patterns. These patterns could be reversed by cooling the surface, enabling flexible control over wetting properties. This platform allowed the formation of on-demand droplet guiding pathways and spatiotemporal droplet manipulation within seconds, showcasing its potential for advanced applications in programmable liquid handling.

For applications where minimal disruption to background flow fields is essential (e.g., biomedical systems), metamaterial-inspired surfaces offer a novel solution [51]. These artificial materials possess unique properties, such as invisibility, field rotation, and field concentration. Chen et al. integrated pillar arrays into a microfluidic platform, simulating a porous cloak that redirected flow while maintaining environmental stability [52]. Such designs hold potential for next-generation fluidic cloaking and stealth transport.

26884062, 2026, 2, Downloaded from https://onlinelibrary.wiley.com/doi/10.1002/sstr.202500492 by Scholarly Resource Services, Wiley Online Library on [04/11/2026]. See the Terms and Conditions (https://onlinelibrary.wiley.com/terms-and-conditions) on Wiley Online Library for rules of use; OA articles are governed by the applicable Creative Commons License

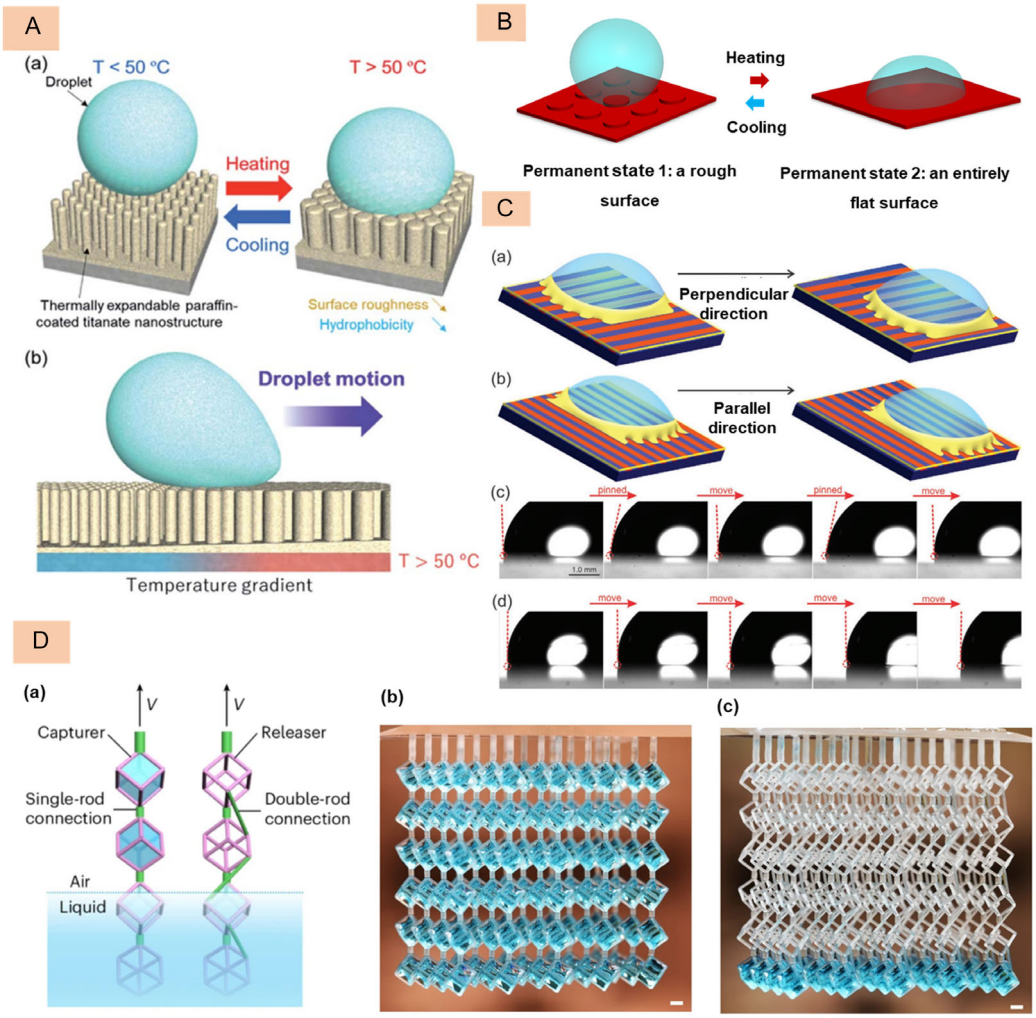


FIGURE 3 | Schematics illustrating examples of engineered micropatterned surfaces with unidirectional wetting property. (A) (a) Wettability alterations of a thermo-responsive paraffin-coated titanate nanorods surface structure induced by changes in surface roughness associated with thermal expansion of paraffin. (b) Droplet motion by spatially heating the substrate. The droplet moves from cold to hot areas owing to the thermocapillary effect. Reproduced with permission from [43], Copyright 2020, Royal Society of Chemistry (RSC). (B) A thermo-responsive micropillar-arrayed LCE surface with reversible/switchable roughness between a high and a completely zero, smooth state. Redrawn with modification from [44], Copyright 2021, Springer. (C) Schematic illustrations of droplet transport on LCHet (lubricated chemically heterogeneous) surface along (a) perpendicular and (b) parallel directions. Moving droplets on the structure along (c) perpendicular and (d) parallel directions, demonstrating stick-slip and uniform movement, respectively. Reproduced with permission from [45], Copyright 2021, Wiley-VCH. (D) (a) Schematic view of two types of CPFs (capturer and releaser). When they are lifted out of the liquid, the single-rod capturer retains the liquid, while the double-rod releaser releases the liquid. Optical images of the 3D liquid array made from (b) capturer and (c) releaser structures. Scale bars, 2 mm. Reproduced with permission from [46], Copyright 2024, Nature.

A new platform of connected polyhedral frames (CPFs) was designed to enable switchable fluid capture and release with spatial and temporal control for precise liquid handling [46]. The dual functionality of the structure, acting either as a liquid capturer or a releaser, was achieved by defining two distinct platform geometries: the single-rod frame and the double-rod frame. Figure 3D shows the schematic illustration of the CPF platform and the dual functionality of the structures. When lifted from water, the single-rod frame demonstrated liquid capture. In this case, capillary forces dominated gravitational forces, allowing water to rise and be retained within the frame. In contrast, the double-rod frame exhibited liquid release, where gravity prevailed and water drained from the structure. The mechanism underlying the single-rod capturing platform is attributed to capillary forces arising from the interaction between the liquid and the hydrophilic frame surfaces. Here, the connecting rod served purely as a mechanical linkage, without providing a drainage pathway for liquid between frames. On the other hand, in the double-rod frame, a liquid film formed between the two rods. This film facilitated a continuous connection between the liquid retained in the structure and the bulk liquid below, ultimately driving drainage.

3 | Design Considerations for Surfaces with Unidirectional Wetting Properties

3.1 | Underlying Mechanism of Liquid Transport

A liquid droplet is stabilized by surface tension, its interaction with a solid surface depends on the balance of interfacial energies at the solid–liquid, liquid–air, and solid–air boundaries. This

26884062, 2026, 2, Downloaded from https://onlinelibrary.wiley.com/doi/10.1002/sstr.202500492 by Scholarly Resource Services, Wiley Online Library on [04/11/2026]. See the Terms and Conditions (https://onlinelibrary.wiley.com/terms-and-conditions) on Wiley Online Library for rules of use; OA articles are governed by the applicable Creative Commons License

relationship is commonly expressed through Young's equation, which relates the contact angle of the droplet to these interfacial tensions. [53] Differences in contact angle across a droplet, known as contact angle hysteresis, generate an unbalanced force. [54] If this force surpasses the resistance caused by pinning, the droplet begins to move. Such motion is linked to differences in Laplace pressure across the curved droplet interface, which may be induced by factors such as gradients in surface chemistry or wettability, micro- or nanoscale surface features, or external fields and stimuli. The driving force comes from the system's tendency to minimize its free energy. Liquid droplet on a patterned surface adopts the configuration that minimizes the sum of solid–liquid, liquid–vapor, and solid–vapor interfacial energies. [55]

3.2 | Surface Engineering for Unidirectional Liquid Transport

To engineer anisotropic surfaces capable of unidirectional liquid transport, several key design criteria must be considered. As summarized in Figure 4, these considerations vary significantly between active and passive transport strategies. The selected approach influences not only the required fabrication techniques and surface morphology but also impacts power requirements, response time, surface complexity, directional precision, and scalability. In general, effective liquid manipulation requires the following: 1) reliable and energy-efficient directional transport, 2) precise and responsive control over liquid movement, 3) fabrication methods that are scalable and cost-effective, and 4) minimal reliance on external equipment or complex infrastructure.

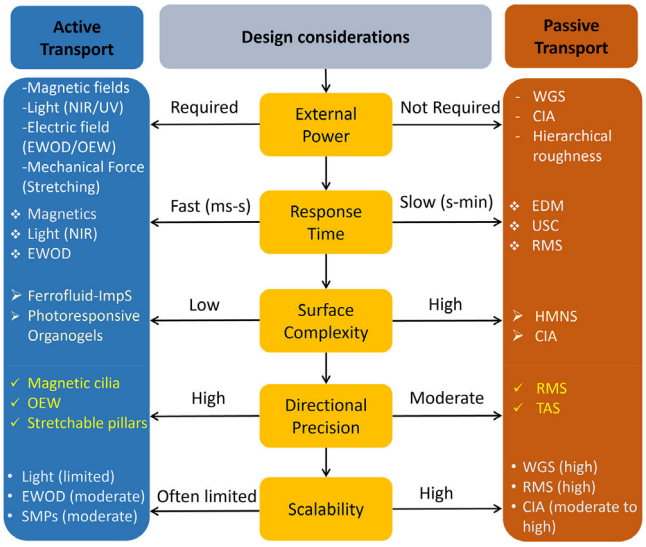


FIGURE 4 | Comparison of active and passive liquid transport mechanisms based on key design considerations: external power, response time, surface complexity, directional precision, and scalability. Full definitions of the abbreviated terms: NIR (Near InfraRed), UV (Ultra Violet), EWOD (Electrowetting-on-Dielectric), OEW (Orbital Electrowetting), ImpS (Impregnated Surface), SMPs (Shape Memory Polymers), WGS (Wettability Gradient Surface), CIA (Curvature-Induced Anisotropy), EDM (Evaporation-Driven Motion), USC (Unidirectional Surface Chemistry), RMS (Ratchet-like Micropatterned Surface), HMNS (Hierarchical Micro/Nanostructured Surface), and TAS (Topographic Asymmetric Surface).

Active transport systems, such as those actuated by magnetic fields, electric fields, light, or mechanical stretching, offer high directional precision and fast response times but typically require external power sources. Representative examples include ferrofluid-impregnated surfaces, photoresponsive organogels, magnetic cilia, and stretchable pillars.

In contrast, passive transport strategies utilize intrinsic surface features, such as chemical gradients, hierarchical roughness, or asymmetric structures, to drive droplet movement without external actuation. While passive surfaces are generally more scalable and energy-efficient, they may offer lower responsiveness and directional control compared to active systems.

The following sections will explore these design considerations in greater detail, highlighting how different surface architectures and actuation mechanisms influence the performance and applicability of unidirectional wetting surfaces.

3.2.1 | Active Transport Methods

Active liquid manipulation relies on external stimuli to achieve precise, dynamic control over liquid transport. In recent years, stimuli-responsive surfaces have become an effective means of controlling liquid movement by combining microstructured features with external stimuli. In this section, we focus on systems where patterned surfaces, such as micropillars or artificial cilia, are not just passive elements but are actively involved in guiding droplets when triggered by light, magnetic fields, or electrical signals. Rather than looking at surface chemistry alone, we specifically highlight cases where surface patterning and responsiveness work together to enable directional transport.

These methods typically use magnetic fields, light (NIR/UV), electric fields (e.g., electrowetting-on-dielectric (EWOD) or orbital electrowetting (OEW), or mechanical deformation (such as stretching) to guide liquid behavior in real time. They enable rapid response times, typically in the millisecond to second range, and provide high directional precision, even under challenging conditions such as manipulating viscous liquids or achieving rapid droplet switching [56, 57]. However, active methods have several limitations, as summarized in Figure 4. For example, external power input is generally required to activate the responsive elements, and scalability may be constrained due to the complexity of materials, fabrication processes, or system integration.

Based on their underlying mechanism, active strategies can be grouped into two main design categories:

i Surface modification with stimuli-responsive materials, where external triggers modulate wettability. Examples include the following: ferrofluid-impregnated surfaces (ImpS) that respond to magnetic fields [19], photoresponsive organogels that guide droplets under NIR irradiation, thermally responsive surfaces with poly(N-isopropylacrylamide) (PNIPAM)-coated Janus silicon micropillars [58], and

26884062, 2026, 2, Downloaded from https://onlinelibrary.wiley.com/doi/10.1002/sstr.202500492 by Scholarly Resource Services, Wiley Online Library on [04/11/2026]. See the Terms and Conditions (https://onlinelibrary.wiley.com/terms-and-conditions) on Wiley Online Library for rules of use; OA articles are governed by the applicable Creative Commons License

light-responsive azobenzene liquid crystal polymer (LCP) films [42].

ii Dynamically reconfigurable surface structures, where surface morphology changes in response to external force fields. These include the following: magnetic artificial cilia for low-adhesion transport, OEW for programmable directional control, and **s**tretchable pillars and shape memory polymers (SMP)-based surfaces that switch between adhesive and nonadhesive states [59, 60].

These categories are elaborated in the following subsections.

3.2.1.1 | Modified Micropatterned Surfaces with Responsive Materials

3.2.1.1.1 | Magnetically Responsive Surfaces. Many studies have focused on developing smart magnetic-responsive surfaces for liquid manipulation. Magnetic fields offer several advantages for droplet transport, including convenience, wireless control, robustness, spontaneous response, and good biocompatibility [61]. However, paramagnetic droplets require functionalization to become magnetic, and handling diamagnetic fluids like water through a magnetic field is particularly challenging, as it demands extremely strong magnetic fields, often requiring superconducting magnets.

To address this issue, Khalil et al. proposed a lubricant-impregnated surface, where the solid texture was impregnated with ferrofluid, a colloidal suspension of ferromagnetic nanoparticles in an oil-based carrier fluid [19]. In the absence of a magnetic field, the nanoparticles were randomly oriented. When a magnetic field was applied, the magnetic dipoles aligned with the field, exhibiting strong magnetic interactions. This method enabled the transport of various fluid types, including diamagnetic liquids, with relatively small magnetic fields through covering the droplet with a thin ferrofluid layer, making the droplet magnetic. The oil-based ferrofluid, being immiscible with water, allowed water droplets to move stably on the surface.

In nature, many microorganisms use motile cilia to control their movement [62–65]. Inspired by these structures, magnetically driven artificial cilia have been developed to enable directional droplet motion [66, 67]. Ben et al. designed a superhydrophobic magnetic microcilia array (MMA) by combining the concepts of motile cilia, the superhydrophobicity of lotus leaves, and the migratory behavior of pigeons [68]. This low-adhesion surface allowed for precise droplet manipulation in both air and underwater environments. Droplets moved freely when an external magnetic field was applied, with their transport speed adjustable by altering the magnet's speed. Results showed that droplet transport depends on the microcilia characteristics and magnetic field strength but not the droplet size.

Chen et al. developed a magnetically responsive superhydrophobic PDMS (MRS-PDMS) surface featuring an outermost layer of microcilia structures [69]. These microcilia enhanced surface strength, long-term stability, and superhydrophobicity. They acted as support to minimize adhesion between the film and water droplets and provided structural robustness through in situ formation. Under an external magnetic field, the surface deformed rapidly, enabling precise droplet manipulation. This multifunctional surface facilitated parallel droplet manipulation and serial dilution, demonstrating its versatility for advanced applications (see Figure 5A).

Yang et al. introduced a smart magnetically responsive superhydrophobic surface featuring a dense array of magnetorheological elastomeric micropillars embedded with dispersed iron particles [70]. By applying and removing an external magnetic field, the surface could reversibly transition between water-repellent and water-adhesive states, as shown in Figure 5B. The adjustable stiffness of the elastomer pillars enabled morphological changes between collapsed and upright positions under the influence of the magnetic field. In the absence of a magnetic field, the soft micropillars bent under the droplet's weight, creating a large contact area, resulting in a hydrophobic adhesive state. When the magnetic field was applied, the micropillars stiffened and oriented vertically, reducing the droplet's contact area to only the pillar tips. This transition shifted the surface to a superhydrophobic, low-adhesion state. The surface's adhesion and sliding behavior were shown to depend on the magnitude of the magnetic force and the composition ratios of PDMS, iron particles, and solvent used in the fabrication process.

Magnetically driven droplet manipulation offers several distinct advantages, including noninvasiveness, independence from droplet properties, rapid responsiveness, and excellent biocompatibility [74, 75]. However, challenges such as contamination of magnetic particles, additional phase extraction processes, and reagent storage and transport must be addressed in future developments.

3.2.1.1.2 | Other External Stimuli-Responsive Surfaces. In addition to magnetism, other external stimuli such as light, temperature, and electricity can be used to control droplet motion directionally. Among these, light holds significant promise for applications in physics, chemistry, and biology, due to its noncontact manipulation capabilities, excellent spatial and temporal resolution, and compatibility with biological systems [76]. Light-driven liquid transport can be achieved through various methods, including modifying surfaces with photoswitchable chemical compounds, incorporating light-responsive materials into liquids, and using light-activated polymers [77]. For example, Gao et al. developed a photoresponsive organogel surface (POS) by embedding Fe_3O_4 nanoparticles into PDMS and infusing it with lubricant [78]. Droplet manipulation was achieved by triggering the surface with NIR (near-infrared) irradiation, which created localized dynamic temperature gradients in the irradiated areas. These gradients allowed droplet transport along desired pathways with controllable velocity and direction. Similarly, Shun et al. utilized light to control the configurations of nanostructured surfaces, guiding both static and moving droplets through channels [79]. Another approach involves photoinduced asymmetric deformation of photo-responsive materials in tubular micro-actuators [80]. This technique allows liquid slugs inside microchannels to move spontaneously due to the capillary forces generated by the reorientation of the photo-responsive material.

Despite the advantages of light-driven liquid transport, some limitations still exist [81]. For instance, optical systems tend to be bulky and complex, which hinders their integration into

26884062, 2026, 2, Downloaded from https://onlinelibrary.wiley.com/doi/10.1002/sstr.202500492 by Scholarly Resource Services, Wiley Online Library on [04/11/2026]. See the Terms and Conditions (https://onlinelibrary.wiley.com/terms-and-conditions) on Wiley Online Library for rules of use; OA articles are governed by the applicable Creative Commons License

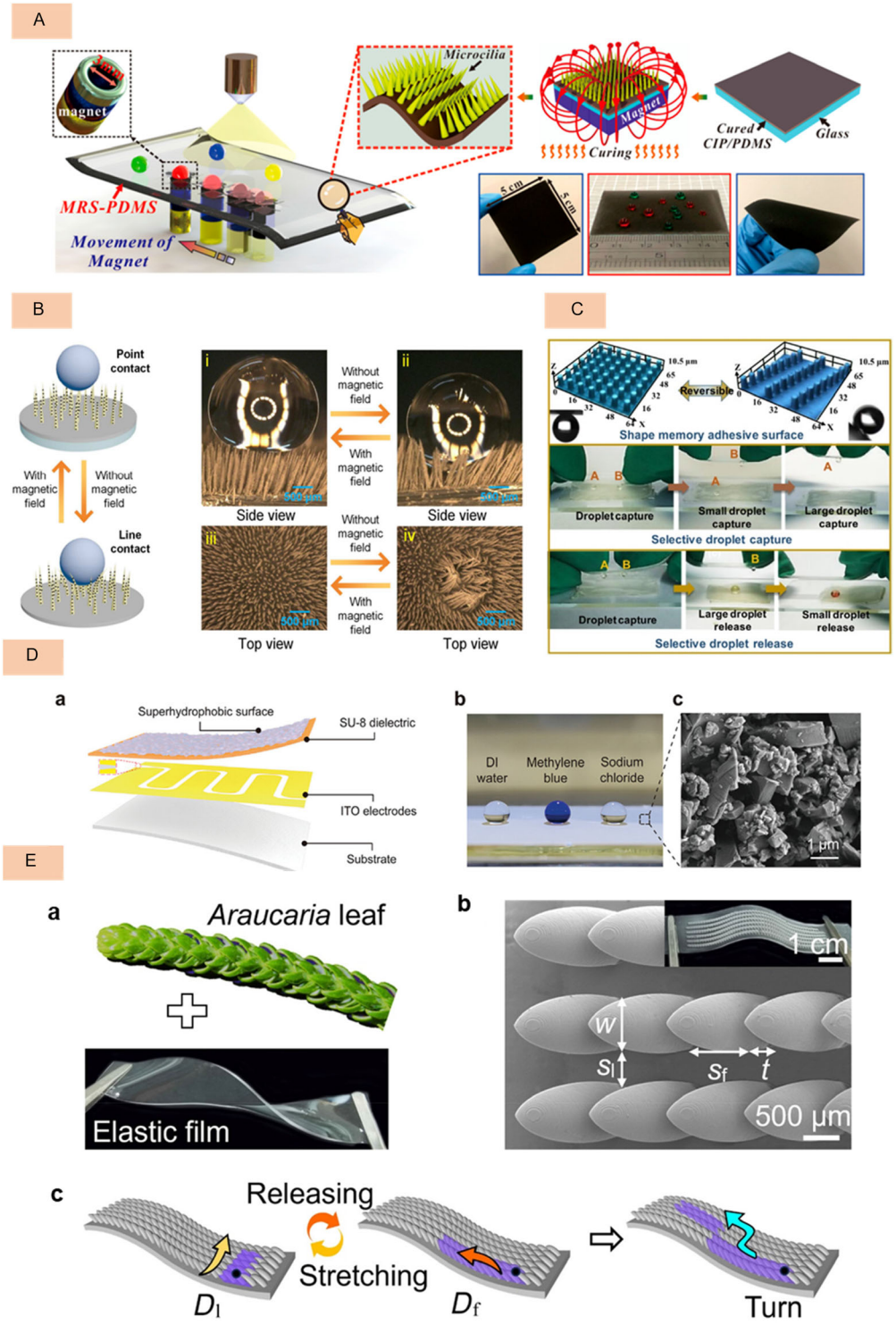


FIGURE 5 | Examples of micropatterned surfaces for active liquid manipulation. (A) (a) Magnetically driven droplet manipulation is enabled with magnetically responsive superhydrophobic PDMS (MRS-PDMS) surface covered with a layer of microcilia (b) Optical images of the flexible MRS-PDMS film, the dye droplets maintain their spherical shape. Reproduced with permission from [69], Copyright 2021, American Chemical Society (ACS). (B) (a) Schematic illustration of reversible switching of the adhesion and wettability of magnetically responsive superhydrophobic surface comprising of a dense array of magnetorheological elastomeric micropillars (b) Microscopic images indicating the reversible changes of the magnetorheological elastomeric micropillars affected by an external magnetic field, from collapsed (adhesive state) to fully upright state (repelling state). Reproduced with permission from [70], Copyright 2018, American Chemical Society (ACS). (C) Schematic illustration of a superhydrophobic shape memory adhesive surface, obtained by sticking a pillar arrayed superhydrophobic polyurethane layer onto a shape memory polyurethane–cellulose nanofiber film. Reproduced with permission from [71], Copyright 2019, American Chemical Society (ACS). (D) (a) Schematic of the structural design of the OEW. (b) State of droplets from different liquids on the surface of the design. (c) SEM image of the dual-scale structure of the superhydrophobic surface. Reproduced with permission from [72], Copyright 2024, Wiley-VCH. (E) (a) Design concept of TELD. (b) Scanning electron microscopy (SEM) image of the TELD with an array of ratchets. (c) Schematic of the fluid manipulation capability of TELD. Reproduced with permission from [73], Copyright 2025, American Association for the Advancement of Science (AAAS).

26884062, 2026, 2, Downloaded from https://onlinelibrary.wiley.com/doi/10.1002/sstr.202500492 by Scholarly Resource Services, Wiley Online Library on [04/11/2026]. See the Terms and Conditions (https://onlinelibrary.wiley.com/terms-and-conditions) on Wiley Online Library for rules of use; OA articles are governed by the applicable Creative Commons License

miniature systems. Additionally, the potential heating effect of droplets caused by optical energy needs to be minimized.

Furthermore, electrowetting on dielectric surfaces (EWOD) has proven to be an effective strategy for droplet manipulation in lab-on-a-chip applications, supporting processes such as dispensing, mixing, splitting, and transporting [82]. An electric field can manipulate droplet motion on both air and water surfaces [83]. For example, droplet transport has been studied using a superhydrophobic surface as a counter electrode, with an applied voltage [84]. The results revealed several advantages, including a 30% reduction in applied voltage and a 30% increase in average speed compared to classical systems, with a maximum instantaneous speed of 460 mm/s. This method allows for better control of the droplet's direction and movement path [77]. Electrowetting also has the benefits of low energy consumption, fast response time, and scalability. However, it requires the complex construction of electrical circuits, high-voltage sources, and electrodes [85–87].

In a recent study by Tan et al., droplet manipulation was achieved on superhydrophobic surfaces using orbital electrowetting (OEW) [72]. The OEW structure follows a sandwich-style configuration, comprising a superhydrophobic surface, an SU-8 dielectric layer, a pair of indium tin oxide (ITO) electrodes, and a substrate from top to bottom, as shown in Figure 5D. The dual-scale properties of the superhydrophobic surface minimize the contact area, enabling a low-resistance droplet transport mode. Directional manipulation was achieved through an asymmetric electrowetting force generated by the tapered orbit, allowing precise control of droplet speed and direction. The platform demonstrated high-speed droplet transport (−210 mm/s), including the ability to climb upward against gravity on a surface with a 55° angle, with durable functionality. Furthermore, the technique proved effective for various types of liquid droplets, including acids, bases, salts, organics (e.g., methyl blue), and artificial blood, in a contaminant-free manner.

3.2.1.2 | Tunable Wettability under External Stretching and Deformation. As mentioned above, surface wettability and adhesion can be dynamically adjusted by stretching or deforming the surface with external forces. As demonstrated by Vu et al., the surface free energy and wettability of the PDMS micropillar array structure could be tuned through applied stretching and releasing cycles [88]. Their findings indicated that stretching resulted in increased surface wettability, thereby decreasing the measured water contact angle values. Wu et al. reported a smart surface with reversibly switchable wetting properties, transitioning from isotropic to anisotropic states using a flexible cylindrical superhydrophobic pillar array [59]. The curvature of a thin cylinder beneath the surface enables tuning of the wetting properties, switching from a pinned (high adhesion) state to a moving mode (low adhesion).

Utilizing additives is a common strategy for on-demand droplet manipulation. Seo et al. developed a stretchable superhydrophobic surface consisting of an array of micropillars [60]. Droplet motion was precisely controlled by creating local dimples on the surface. While the adhesive force between the droplet and the superhydrophobic surface was uniform across the as-prepared flat surface, positive and negative curvatures were created by applying a vacuum beneath the surface. The local deformation allowed the droplet to move toward the created dimple. The team demonstrated that this technique could be used for droplet motion, mixing, or merging.

Anisotropic wettability was also observed on wrinkled polymer surfaces formed through mechanical instabilities such as stretching and releasing. Lee et al. reported a method to tune anisotropic wetting properties by modifying the roughness of wrinkled surfaces [28]. The PDMS substrate was stretched and then exposed to ultraviolet-ozone treatment before being released. The mismatch in elasticity between the soft PDMS substrate and the stiff silicate-like top layer led to the formation of wavy microstructures on the surface. Afterward, SiO_2 nanoparticles and (tridecafluoro-1,1,2,2-tetrahydrooctyl)dimethylchlorosilane were deposited to render the surface hydrophobic. As a result, increasing surface roughness led to a transition from anisotropic/pinned to anisotropic/rollable to isotropic/rollable states.

Among the diverse materials used to fabricate directional wetting surfaces, shape-memory polymers (SMPs) have shown exceptional potential for tuning surface properties. Once deformed, SMPs can retain their surface structures and later return to their original shape. This unique feature makes SMPs ideal for directional droplet manipulation under stretching and deformation [89–91]. These substrates are versatile for various applications [92, 93]. Wang et al. reported a superhydrophobic shape-memory adhesive surface [71], as shown in Figure 5C. The surface was fabricated by bonding a pillar-structured superhydrophobic polyurethane layer onto a shape-memory polyurethane–cellulose nanofiber (PU-CNF) layer. Due to the excellent shape-memory properties of the PU-CNF layer, these surface structures could memorize and provide various microstructure patterns throughout the stretching/releasing process. The team demonstrated reversible adhesive states, switching from a high-adhesion pinned state to a low-adhesion rolling state. These shape-memory structures enable the surface to selectively capture and release microdroplets.

A topological elastic liquid diode (TELD), combining an Araucaria leaf–inspired ratchet array with the elasticity of silicone rubber (Figure 5E a, b), was fabricated for flow-direction manipulation [73]. On the unstretched TELD platform, ethanol (used as the model liquid) predominantly spread in the D_f and L_f directions, with minimal lateral spreading along D_1 and L_1. When tensile stress was applied, producing 50% elongation, the flow direction shifted toward D1 (see Figure 5E c). Upon release of the stress, the condition reverted to the initial state, with flow redirected back to D_f. Thus, reversible flow regulation was successfully achieved through strain-induced manipulation of the TELD's supporting layer.

3.2.2 | Passive Transport Methods

Passive droplet manipulation involves controlling droplet behavior without external actuation or controller interference. This approach offers several advantages, such as precise control over droplet shape, position, and the ability to manipulate multiple droplets without external stimuli [87, 94]. Passive manipulation is primarily achieved by creating wettability gradients through heterogeneous chemical and/or physical modifications [95].

26884062, 2026, 2, Downloaded from https://onlinelibrary.wiley.com/doi/10.1002/sstr.202500492 by Scholarly Resource Services, Wiley Online Library on [04/11/2026]. See the Terms and Conditions (https://onlinelibrary.wiley.com/terms-and-conditions) on Wiley Online Library for rules of use; OA articles are governed by the applicable Creative Commons License

Its effectiveness can be further enhanced by designing anisotropic surface structures, such as liquid diodes with reentrant microstructures. Depending on the geometry, gravitational or capillary forces can trigger fluid motion. Similar principles are also exploited in passive microfluidic systems, where geometric asymmetry and inertial effects can guide cell or particle movement without external actuation [96]. This section briefly reviews the general design considerations of these techniques. A more detailed discussion on the design principles and mechanics of droplet transport based on wettability modulations is available in a recent review paper [94].

3.2.2.1 | Micropatterned Surfaces with Wettability Contrast Property. The simplest approach involves creating wetting contrasts by fabricating alternating hydrophilic patterns on a superhydrophobic substrate. Gravitational forces can then induce directional droplet movement. Using this technique, Chang et al. developed a gravity-induced droplet sliding platform with hydrophilic/superhydrophobic patterned surfaces for nanoliter-sized droplet deposition [97]. This system allowed for the simultaneous deposition of multiple liquid drops. As shown in Figure 6A, droplets of different liquids were initially placed on the first row of hydrophilic pads. When the surface was tilted, gravity caused the droplets to slide, with their rear edges repeatedly experiencing pinning and depinning states during the sliding process.

Similarly, Zhang et al. created a microscale fractal superhydrophobic surface patterned with hydrophilic microchannels [99]. The combination of physical groove structures and localized surface energy differences between regions inside and outside the grooves produced anisotropic sliding behavior. In the direction

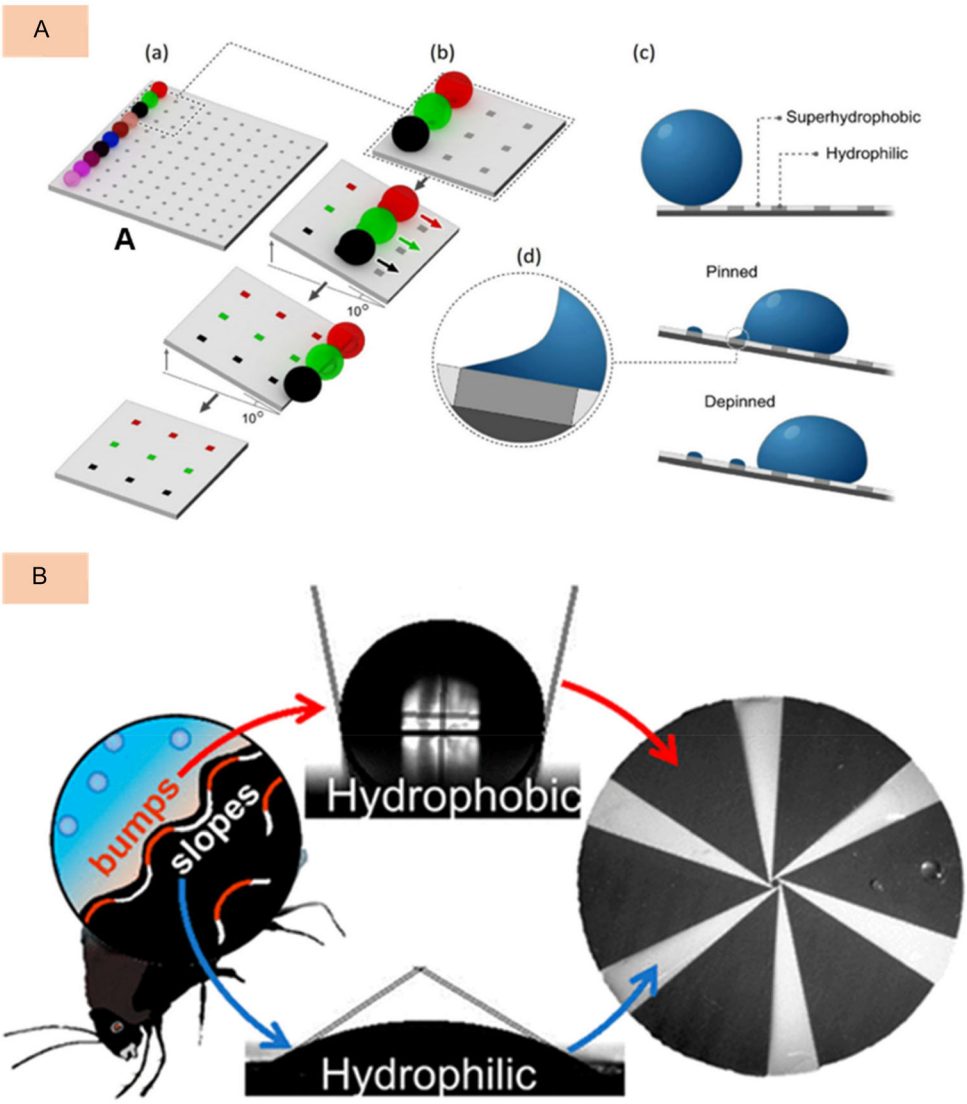


FIGURE 6 | Examples of surfaces with wettability contrast property for passive liquid manipulation. (A) A gravity-induced droplet sliding platform using hydrophilic pads on a superhydrophobic substrate: (a) Different types of liquid droplets are positioned on the first row of an array of hydrophilic pads. (b) Magnified view of droplet sliding procedure. (c) Side view of a droplet sliding procedure. (d) Magnified view of the rear edge of the droplet contact line pinned on the hydrophilic region. Reproduced with permission from [97], Copyright 2016, American Institute of Physics (AIP). (B) Schematic of the design of the Namib desert beetle-inspired contrast wettability surface. Reproduced with permission from [98], Copyright 2023, American Chemical Society (ACS).

26884062, 2026, 2, Downloaded from https://onlinelibrary.wiley.com/doi/10.1002/sstr.202500492 by Scholarly Resource Services, Wiley Online Library on [04/11/2026]. See the Terms and Conditions (https://onlinelibrary.wiley.com/terms-and-conditions) on Wiley Online Library for rules of use; OA articles are governed by the applicable Creative Commons License

parallel to the hydrophilic channels, the droplet sliding angle was less than 10°. However, droplets moving perpendicular to these channels encountered relatively high sliding angles due to contact line pinning. Once tilted, droplets moved steadily along predefined stripe structures. These stripe-shaped structures could be fabricated in various geometries, including straight, curved, or S-shaped designs. Inspired by the Namib Desert beetle, a textured surface was designed with alternating hydrophobic and hydrophilic patterns to control droplet transport on an aluminum alloy substrate, as shown in Figure 6B [98].

The hydrophobic regions were created using a durable fluorine-based polymer powder coating, while the hydrophilic sections were achieved through femtosecond laser texturing. Droplet transport relies on two primary mechanisms: the transition of droplets from hydrophobic to hydrophilic regions and capillary-driven outward radial fluid flow along the hydrophilic tracks. By placing droplets at the hydrophilic-hydrophobic junction, droplets with volumes of up to 50 μL could be transported along a single hydrophilic track, leaving the hydrophobic regions free of wetting traces.

3.2.2.2 | Surfaces with Distinctive Physical Structural Shapes. Passive fluid manipulation can also be achieved by designing unique geometries with wettability gradients that leverage capillary forces for transport. For instance, Soltani and Golovin demonstrated the passive transportation of low surface tension (LST) liquids over a long distance (over 150 mm) [21]. The main challenge, minimizing the contact line resistance, was overcome by using two distinct liquid-like polymer brushes for the channel and background substrate. Upon deposition of an LST droplet at the channel entrance, its bulged shape and the asymmetrical wedge geometry created Laplace pressure, enabling droplet spreading. This design facilitated droplet splitting, merging, mixing, and guided movement through curves, corners, and complex patterns for various LST liquids.

Liu et al. developed a microanisotropic superhydrophobic surface (MATS) featuring periodic isosceles triangle microarrays coated with nanoporous alumina for superhydrophobicity [100]. This surface allowed self-powered, long-distance, direction-controlled droplet manipulation. The anisotropic liquid-solid adhesion drove microdroplets to leap along the surface. Liquid diodes represent another example of anisotropic surfaces tailored for unidirectional liquid transport. Analogous to electronic diodes, liquid diodes minimize resistance in one direction while creating high resistance in the opposite direction [101]. As reported by Li et al., a liquid diode with reentrant surface topography and U-shaped island arrays enclosed by patterned fences facilitated fast, directional, long-distance liquid transport [102]. The U-shaped cavities featured reentrant structures to prevent backflow, making this design ideal for efficient passive droplet manipulation. Figure 7A illustrates the concept. Li et al. have extensively reviewed design parameters for various liquid diode structures [105].

The unidirectional flow of liquids holds significant potential in microfluidic devices, particularly in applications such as micromixers. One notable innovation in this field is the introduction of Tesla valve structures as micromixers [103]. Wang et al. demonstrated that using a Tesla valve micromixer eliminates the need for additional equipment traditionally required to impose one-way flow, which was a key component in

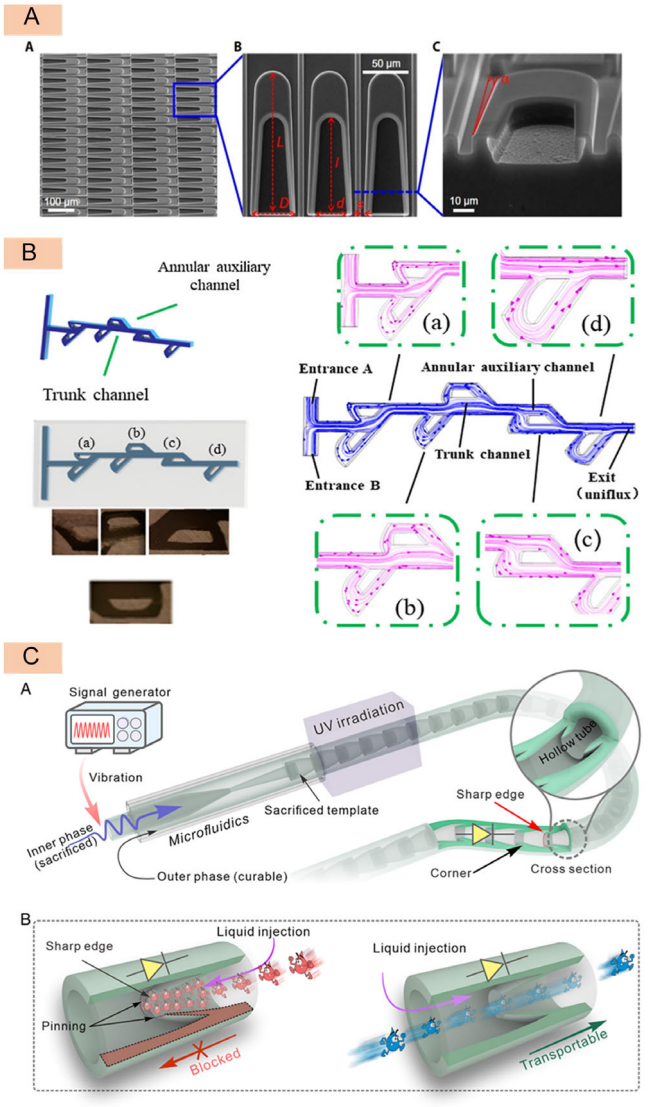


FIGURE 7 | Examples of surfaces with distinctive physical structural shapes for passive unidirectional liquid manipulation (A) (a) SEM image of the designed liquid diode structure. (b) SEM image of U-shaped island array with the re-entrant cavity on one side. As shown, L and D represent the length and width of the island, l and d represent the length and width of the cavity, and s is the opening width of the divergent side channel. (c) Zoomed cross-sectional view of the re-entrant structure at the interior wall of the cavity. α is the apex angle of the diverging side-channel. Reproduced with permission from [102], Copyright 2017, American Association for the Advancement of Science (AAAS). (B) Schematic of the structural design of AAC. (a–d) Zoomed view of different sections of the structure. Reproduced with permission from [103], Copyright 2022, American Chemical Society (ACS). (C) A Schematic illustration of the design structure and preparation process of the flexible liquid-diode microtube. B Schematic of unidirectional fluid transport into the flexible liquid-diode microtube, Reproduced with permission from [104], Copyright 2024, National Academy of Sciences.

conventional designs [103]. As shown in Figure 7B, the unique morphological structure of the Tesla valve facilitates unidirectional fluid flow, enhancing mixing efficiency. Their findings revealed that the 5-AAC (annular auxiliary channel and trunk channel) Tesla valve micromixer significantly outperformed

26884062, 2026, 2, Downloaded from https://onlinelibrary.wiley.com/doi/10.1002/sstr.202500492 by Scholarly Resource Services, Wiley Online Library on [04/11/2026]. See the Terms and Conditions (https://onlinelibrary.wiley.com/terms-and-conditions) on Wiley Online Library for rules of use; OA articles are governed by the applicable Creative Commons License

the common T-shaped planar channel, achieving a mixing efficiency of up to 0.89 at a flow rate of 2 ml/min.

To date, research has predominantly focused on developing diode-based unidirectional liquid handling platforms on open surfaces. A major challenge persists in implementing diode-like liquid handling strategies within enclosed platforms. Addressing this, Yang et al. recently designed a flexible diode-like microtube for unidirectional liquid transport within an enclosed chamber [104]. The inner morphology of the microtube, as shown in Figure 7C, features a series of truncated, overlapping cone-shaped microcavities with sharp edges and corners along the tube's axis. This asymmetric morphology imparts diode-like liquid transport properties, enabling unidirectional liquid motion driven by a Laplace gradient and asymmetric pinning effects. Furthermore, the structure's exceptional flexibility, achieved using a dual-network hydrogel composed of poly (ethylene glycol) diacrylate (PEGDA) and calcium alginate materials, makes it ideal for directional liquid manipulation along arbitrary pathways.

4 | Fabrication Methods of Micropatterned Anisotropic Surfaces with Unidirectional Wetting Properties

In this section, various fabrication methods for anisotropic surfaces are presented. The surfaces are categorized based on the type of anisotropy, divided into two main groups: one arising from geometric structures and the other from the chemical properties of the surfaces. For each category, the relevant fabrication techniques are outlined. This classification serves as a practical guideline for identifying suitable fabrication approaches for engineering surfaces with specific anisotropic characteristics. A summary of these fabrication techniques, organized by the type of anisotropy, is shown in Figure 8.

4.1 | Geometrical Anisotropy

In this type of anisotropy, surfaces consist of organized arrays of micro- or nanoscale patterns with geometric features designed to create direction-dependent wetting or adhesion. Various fabrication methods have been used to develop these surfaces for applications requiring direction-regulated droplet manipulation.

4.1.1 | Replica Molding Method

In this strategy, anisotropic micro/nanopatterned wetting surfaces are prepared by replicating the template or mold shape onto target materials. For instance, Zhang et al. used a natural stamp, using PDMS replica molding from the surface of grasshopper wings, to create an anisotropic wetting surface with similar geometric patterns [106]. This approach provides a simple and cost-effective preparation method without requiring expensive or complex equipment.

Li et al. developed a triangular micropillar array surface (TMAS) for droplet manipulation [107]. TMAS consists of a PDMS backing layer and an array of triangular micropillar structures. The fabrication process, illustrated in Figure 9A, involves casting a PDMS precursor into a PDMS mold containing triangular microholes. The mold, filled with the PDMS precursor, is then placed in contact with a prestretched PDMS layer and baked at 90°C for 1 h. Once cured, the triangular micropillar array is obtained by peeling it off the mold, followed by releasing the mechanical stress from the PDMS backing layer.

Another study describes the fabrication of a superhydrophobic shape-memory adhesive surface capable of fixing and memorizing various shape arrangements induced by stretching and releasing processes [71]. This surface consists of two layers: a pillar array of superhydrophobic polyurethane (s-PU) created using a double-casting technique and a shape-memory polyurethane–cellulose nanofiber (PU–CNF) substrate synthesized through solvent casting. The detailed fabrication process is depicted in Figure 9B.

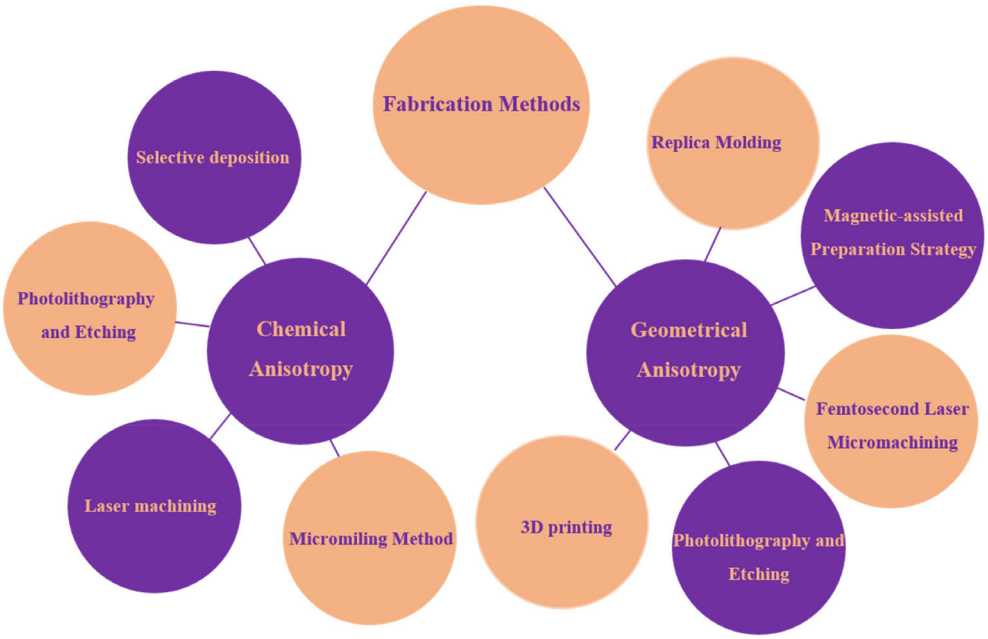


FIGURE 8 | Summary of the fabrication techniques based on the surface's type of anisotropy.

26884062, 2026, 2, Downloaded from https://onlinelibrary.wiley.com/doi/10.1002/sstr.202500492 by Scholarly Resource Services, Wiley Online Library on [04/11/2026]. See the Terms and Conditions (https://onlinelibrary.wiley.com/terms-and-conditions) on Wiley Online Library for rules of use; OA articles are governed by the applicable Creative Commons License

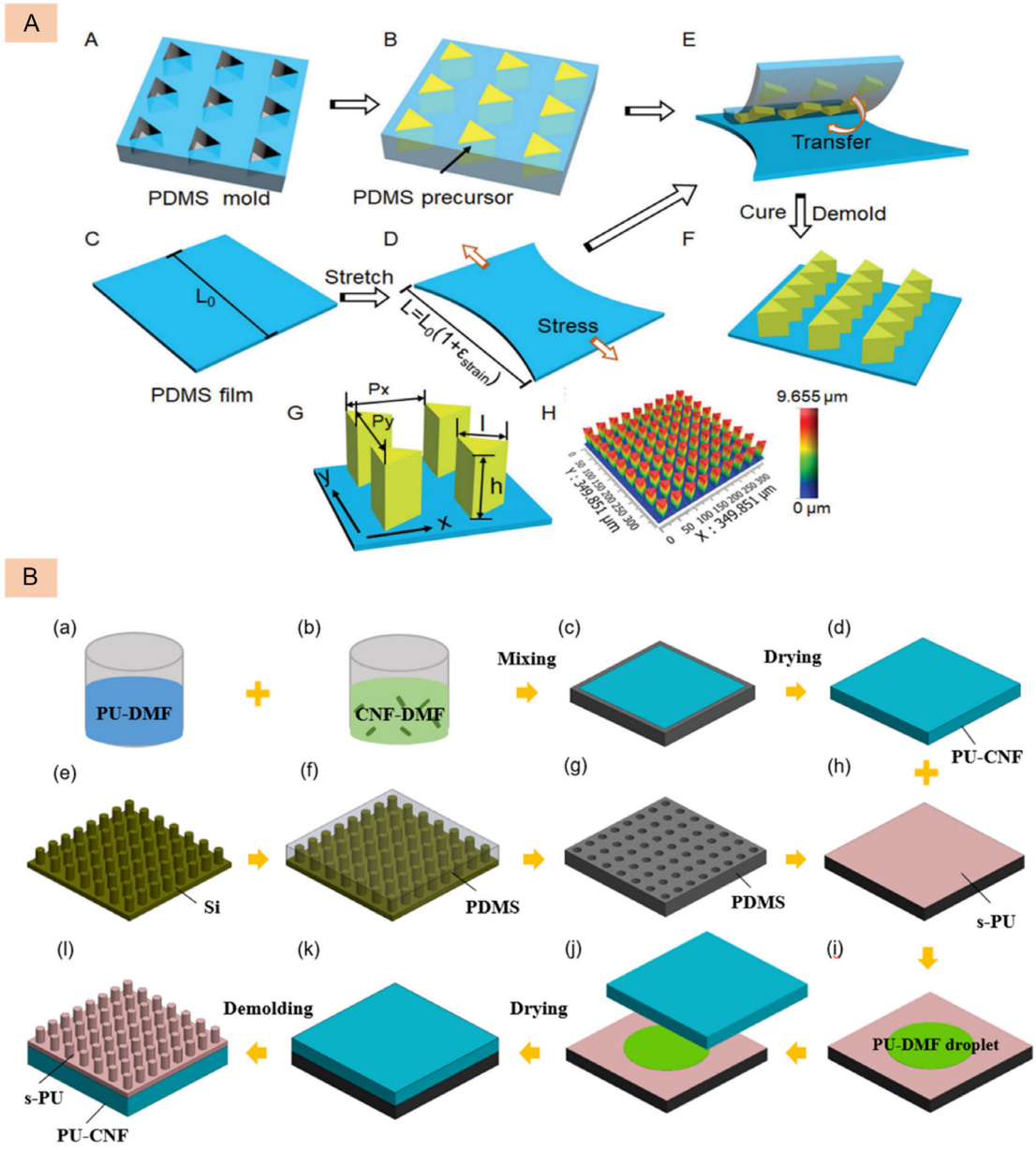


FIGURE 9 | Examples of available fabrication methods for creating micro/nanoscale physically patterned surfaces. (A) Fabrication process of triangular micropillar array surface (TMAS) structure. (a) PDMS mold containing triangular microholes (b). PDMS precursor was cast into the PDMS mold. (c-d) PDMS layer was prestretched in the *x* or *y* direction to a specific strain, ϵ strain. (e) The PDMS precursor-filled mold was placed in contact with a prestretched PDMS layer and then baked at 90°C for an hour. (f) The triangular micropillar array surface became ready to use after peeling off from the PDMS mold and stress relaxation in the backing layer of PDMS. (g) As demonstrated, *h* and *l* are the triangular micropillar height and the side length of the triangular tip, respectively. And *Px* and *Py* represent the periods in the *x* and *y* directions, respectively. (h) A typical 3D image of TMAS with $\epsilon_{strain} = 0$. Reproduced with permission from [107], Copyright 2020, Wiley-VCH. (B) Detailed fabrication of a superhydrophobic shape memory adhesive surface. (a–d) The processes of solvent casting to fabricate the shape memory substrate (PU-CNF). (e-h) The preparation of the s-PU top layer using the molding method. (i-l) The bonding processes of the two layers. Redrawn with some changes from [71], Copyright 2019, American Chemical Society (ACS).

4.1.2 | Magnetic-Assisted Preparation Strategy

The magnetic-assisted fabrication method has proven effective for creating responsive micro/nanostructured wetting surfaces. During the fabrication process, a magnetic field is applied to control the morphology of the micro/nanostructures, which can be tuned dynamically under an external magnetic force. For example, Huang et al. introduced a ferrofluid-molding technique to produce cone-shaped structures with adjustable inclination angles, enabling the anisotropic wetting behavior of microdroplets [108]. In this method, ferrofluid microdroplets served as master molds to form various microstructures, followed by double-casting techniques. The fabrication process, illustrated in Figure 10A, demonstrates the method's versatility, allowing the creation of complex, asymmetrical micropillars by altering the direction of the external magnetic field.

26884062, 2026, 2, Downloaded from https://onlinelibrary.wiley.com/doi/10.1002/sstr.202500492 by Scholarly Resource Services, Wiley Online Library on [04/11/2026]. See the Terms and Conditions (https://onlinelibrary.wiley.com/terms-and-conditions) on Wiley Online Library for rules of use; OA articles are governed by the applicable Creative Commons License

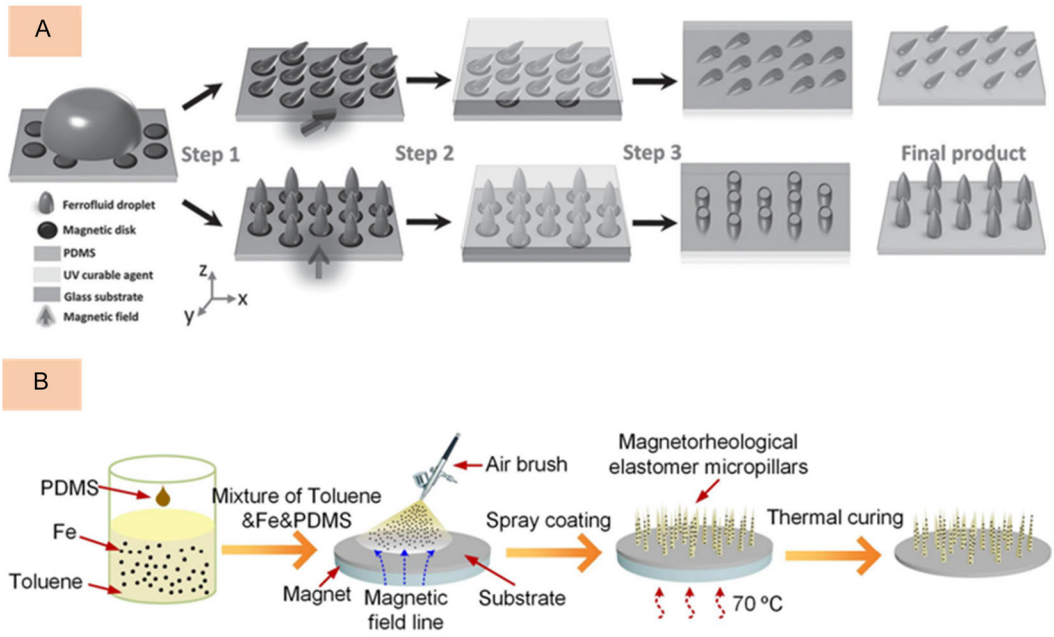


FIGURE 10 | Examples of available fabrication methods for creating micro/nanoscale physically patterned surfaces. (A) An overview of the preparation procedure of cone-shaped PDMS structures based on the magnetic-assisted (Ferrofluid-Molding) method. Ferrofluid microdroplets were created by applying an external magnetic field. Next, UV-curable tri (propylene glycol) diacrylate was cast on the microdroplets to generate the negative mold. Finally, PDMS microcones with various inclination angles, affected by a tilted magnetic field, were created by PDMS casting. Reproduced with permission from [108], Copyright 2015, Wiley-VCH . (B) Schematic view of the preparation mechanism of a smart magnetic-responsive superhydrophobic surface, consisting of an array of magnetorheological elastomer micropillars, through spray-coating and magnetic-field-directed self-assembly. First, a mixture containing toluene solution, PDMS prepolymer, and carbonyl iron particles was prepared. The obtained homogeneous mixture was sprayed onto a structure that was put on a magnet using an airbrush. The mixture instantly oriented along the direction of the magnetic field and generated an array of micropillar structures. After the PDMS is cured, the micropillars' shape and orientations will be fixed. Reproduced with permission from [70], Copyright 2018, American Chemical Society (ACS).

In another study, researchers developed a smart magnetic-responsive superhydrophobic surface with tunable wettability [70]. These surfaces were fabricated by spray-coating a self-assembled solution of PDMS and carbonyl iron particles, as shown in Figure 10B. The wettability of the surface could be adjusted in real time by simply turning the external magnetic field on or off.

4.1.3 | Femtosecond Laser Micromachining

The femtosecond laser micromachining method provides a fast, mask-free, and efficient approach for fabricating micro/nanopatterned surface structures on various materials without requiring clean room facilities [109, 110]. It is also recognized as an emerging tool for creating anisotropic micropatterned surfaces. For instance, Schnell et al. used femtosecond laser micromachining to directly fabricate groove structures on metallic surfaces [111]. These grooves featured a fixed shape with a constant gap width (20 μm) and depth (10 μm), while the strut width varied from 1 to 300 μm. The contact angles in the parallel and perpendicular directions were influenced by the strut width. Furthermore, the ratio of contact angles in these directions decreased with increased hydrophobicity of the groove gap.

In another study, Song et al. combined femtosecond micromachining with a magnetic-assisted preparation technique to fabricate a heterogeneous, high-aspect-ratio, magnetically responsive microcolumn array [34]. The detailed fabrication process is illustrated in Figure 11A.

4.1.4 | Photolithography and Etching

Photolithography and etching are among the most common techniques for fabricating micro/nanopatterned structures. These methods utilize light to transfer the desired pattern from a mask onto a substrate, followed by etching to remove the unprotected areas [113]. Lee et al. introduced a fabrication technique for creating asymmetric grooved structures using photolithography, anisotropic KOH etching, and transfer molding [7]. Initially, two silicon (Si) wafers were patterned using photolithography and anisotropic wet etching with KOH. A PDMS replica was molded on one wafer and then reversibly bonded to the other silicon wafer containing complementary patterns. The microchannel arrays were filled with SU-8 using capillary forces. Finally, the PDMS mold was detached by bonding the SU-8 channels to an adhesive polymer film. This method produced SU-8 asymmetric surface structures with anisotropic wetting properties.

In another study, researchers developed a thin, stretchable, superhydrophobic PDMS surface structure featuring micropillar arrays using lithography, dry etching, and casting [60]. The fabrication began with a Si master mold containing an array of microholes created by photolithography and plasma etching. The Si mold surface was then treated with a superhydrophobic self-assembled monolayer. The micropatterns were transferred onto a PDMS substrate using a casting technique.

26884062, 2026, 2, Downloaded from https://onlinelibrary.wiley.com/doi/10.1002/sstr.202500492 by Scholarly Resource Services, Wiley Online Library on [04/11/2026]. See the Terms and Conditions (https://onlinelibrary.wiley.com/terms-and-conditions) on Wiley Online Library for rules of use; OA articles are governed by the applicable Creative Commons License

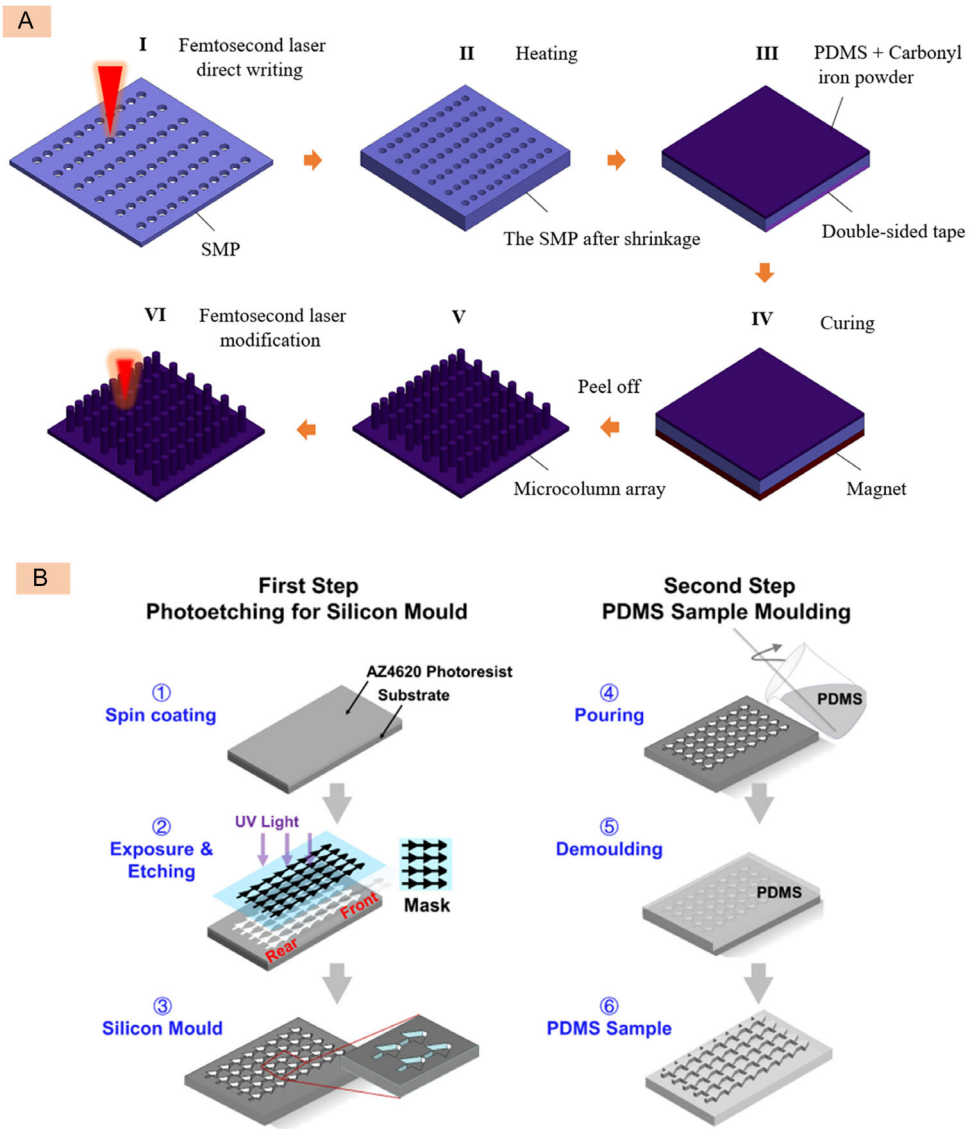


FIGURE 11 | Examples of available fabrication methods for creating micro/nanoscale physically patterned surfaces. (A) Schematic illustration of the fabrication procedure of the high-aspect-ratio magnetically responsive microcolumn array surface structure. (I) First, femtosecond laser micromachining was used to generate high-aspect-ratio microholes on a shape memory polymer (SMP). (II) The SMP surface containing microholes was heated to be shrunk. (III) Next, the PDMS with carbonyl iron powder was poured into the shrunk polystyrene substrate to achieve the microcolumn structure. The double-sided tape was attached to one side of the polystyrene sheet. (IV) A piece of magnet was put under the substrate for a short time to organize the iron particles into chains. After curing the sample, the double-sided tape was removed. (V) Then, the high-adhesive superhydrophobic surface structure was peeled off the mold. (VI) In the end, femtosecond laser modification changed the surface into a low-adhesion superhydrophobic sample. Redrawn with some changes from [34], Copyright 2020, American Chemical Society (ACS). (B) Schematic of the preparation steps of BAMS via the photolithography method followed by PDMS casting. Reproduced with permission from [112], Copyright 2024, American Chemical Society (ACS).

A stretchable branch-shaped asymmetric microstructured surface (BAMS) was fabricated on PDMS for unidirectional oil droplet spreading control [112]. As the first stage of the preparation procedure, the silicon mold was fabricated via photolithography technique. The fabrication steps are illustrated in Figure 11B. To ease mold removal, the substrate was coated with 1H, 1H,2H, 2H-perfluorodecyltriethoxysilane. In the final step, PDMS was cast onto the mold and cured in an oven at 120°C for 2 h. After demolding the PDMS from the master silicon mold, the flexible branch-shaped microstructured surface was successfully obtained.

4.1.5 | 3D Printing

3D printing is an additive manufacturing technique that fabricates 3D prototypes by translating computer-aided design (CAD) inputs into physical objects through layer-by-layer resin deposition. This method provides several advantages over conventional strategies, including cost-effectiveness, achieving simultaneous production of multiple samples, and the capability to create intricate and complex structures [113]. This method has demonstrated significant potential in the development of wetting surfaces in diverse shapes.

26884062, 2026, 2, Downloaded from https://onlinelibrary.wiley.com/doi/10.1002/sstr.202500492 by Scholarly Resource Services, Wiley Online Library on [04/11/2026]. See the Terms and Conditions (https://onlinelibrary.wiley.com/terms-and-conditions) on Wiley Online Library for rules of use; OA articles are governed by the applicable Creative Commons License

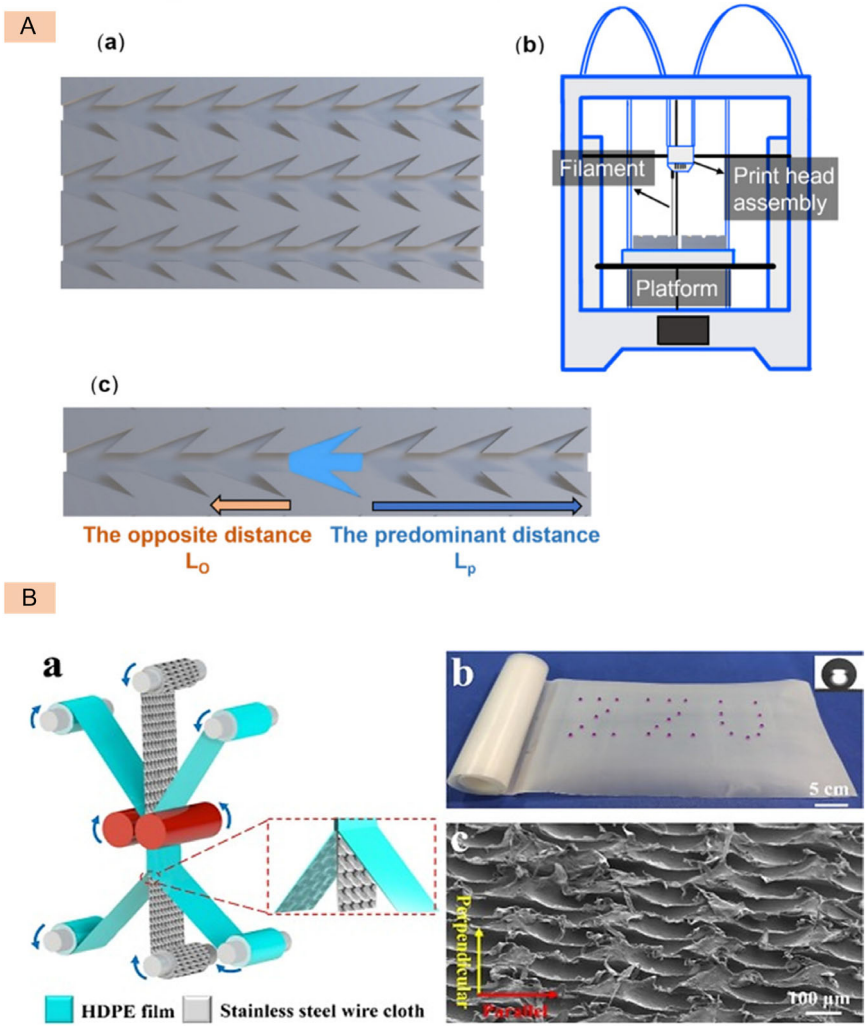


FIGURE 12 | Schematics illustrating examples of available fabrication methods for creating micro/nanoscale physically patterned surfaces. (A) (a) Schematic of dart-shaped patterns. (b) Illustration of the 3D printer machine. (c) Unidirectional fluid flow into microchannel. Reproduced with permission from [114], Copyright 2022, Multidisciplinary Digital Publishing Institute (MDPI). (B) (a) Scheme of development of an organized micropatterned surface on a high-density polyethylene substrate by the roll-to-roll, hot-pressing method. (b) Digital photograph of a roll of H-125 with microdroplets on the micropatterned superhydrophobic surface. (c) SEM image of the micropatterned H-125 morphology. Reproduced with permission from [115], Copyright 2020, Elsevier.

A series of anisotropic, bioinspired dart-shaped groove micropatterns for self-driven unidirectional water transport was prepared using a fused deposition modeling 3D printing technique, followed by surface modification; see Figure 12A [114]. The dart-shaped design induces capillary fluid flow through the main wedge-like structures, while the morphology of the two wedge-like features near the groove's tail obstructs flow in the opposite direction. The design was first created using the CAD software and then imported into the printer. The printing mechanism involved the layer-by-layer deposition of melted solid plastic filaments to create the prototype.

In a recent study by Jiao et al., a rapid 3D printing method was proposed for fabricating soft, ridged-slippery surfaces (SRSSs) with a broad range of anisotropic wettability for droplet manipulation [116]. Initially, an epoxy resin mold was fabricated using a photopolymerization 3D printer. A PDMS mixture was then cast onto the prepared master mold. After thermal curing, the ridged structure was achieved by demolding the PDMS from the 3D-printed master mold. To impart slippery properties, the substrate was immersed in silicone oil, resulting in a 35 μm-thick oil coating on the structure.

4.1.6 | Other Methods

In addition to the mentioned techniques, several strategies have been explored for fabricating micro/nanopatterned anisotropic wetting surfaces. For instance, an anisotropic superhydrophobic surface was fabricated using a homemade melt hot-pressing machine [115]. As shown in Figure 12B, a high-density polyethylene substrate was processed with roll-to-roll hot pressing to produce an organized micropatterned surface. The resulting structure demonstrated low adhesion and exceptional mechanical stability.

Another innovative approach involved creating magnetic soft composite films capable of responding to magnetic fields for reversible control of water droplet adhesion between

26884062, 2026, 2, Downloaded from https://onlinelibrary.wiley.com/doi/10.1002/sstr.202500492 by Scholarly Resource Services, Wiley Online Library on [04/11/2026]. See the Terms and Conditions (https://onlinelibrary.wiley.com/terms-and-conditions) on Wiley Online Library for rules of use; OA articles are governed by the applicable Creative Commons License

rolling and pinning states [47]. The preparation involved coating a mixture of PDMS and carbonyl iron powder onto a coverslip using the doctor-blade method. The film was cured and then soaked in chloroform to dissolve the outermost layer. Before treatment, the surface of the iron-PDMS composite appeared smooth and defect-free. After chloroform treatment, the surface became rough, enhancing its functionality. Table 1 summarizes various studies on fabricating anisotropic surfaces with micro/nanostructures, highlighting the techniques, materials, and key findings.

TABLE 1 | Summary of the studies dedicated to fabricating anisotropic surfaces with micro/nanostructures that can be used for liquid transport.

Structural feature	Control avenue	Fabrication method	Advantages
Slippery and magnetically responsive micropillar array surfaces [117]	External magnetic field	Photolithography and deep reactive ion etching, magnetic-assisted preparation strategy	Presenting quick response and cilia-like beating, which provided directional and continuous small size droplet transport in silicone oil. Polyethylene microbeads transportation in isopropanol through using this platform
A soft magnetic carpet consisting of a set of magnetic-responsive soft hairs, with tunable wettability induced by liquid infusion [118]	External magnetic field	Magnetic-assisted preparation strategy	Providing a platform for sorting and separation of different droplets. Temporal and spatial droplet control result in conducting droplet reactions
A magneto-responsive shutter (MRS) structure composed of an array of microblades fixed on a frame [119]	Magnetic actuation	Laser kirigami and surface modification	Performing two dynamical transforming operations, reversible oscillation and rotation. Providing directional droplet bouncing, distribution, merging, and continuous transportation along straight or curved pathways.
Anisotropic V-shaped prism microarray (VPM) [120]	Thermal stimuli	Photoetching method	Flow direction changing among unidirectional, bidirectional, and reverse unidirectional transportation accomplished by thermal stimuli for on-demand droplet manipulation purposes
A micromechanical device with integrated meshes with double different superwettability tracks (IMDDS) [121]	The wettability can be mechanically adjusted by rotating of a layer of superhydrophilic track and a layer of superhydrophobic track	Etching method	Release and transfer of single or multiple tiny droplets simultaneously in situ. Fast response, low preparation cost, and convenient operation methods
Groove-structured shape-memory polymer (SMP) surface [122]	Alternant pressing and heating treatments	Femtosecond laser direct writing	Repeated switching of surface wettability arising from the inherent properties of shape memory polymer
A digital microfluidic platform based on a shape memory micropillar array [123]	Near-infrared (NIR) light irradiation	Soft lithography and molding method	Capability of the Poly (ethylene-vinyl acetate) (EVA) micropillar array chip in controlled droplet manipulation and detection of ascorbic acid on the chip were demonstrated.
Micro/nanoporous superhydrophobic polytetrafluoroethylene (PTFE) surface [124]	Surface electrical charge-driven droplet manipulation	Carbon dioxide nanosecond pulsed laser ablation	Diverse forms of droplet manipulation such ad fast droplet transportation on the surface with the surface charge density gradient, seeding of the droplet array, and dynamic droplet mixing on designated spots with high surface charge density

26884062, 2026, 2, Downloaded from https://onlinelibrary.wiley.com/doi/10.1002/sstr.202500492 by Scholarly Resource Services, Wiley Online Library on [04/11/2026]. See the Terms and Conditions (https://onlinelibrary.wiley.com/terms-and-conditions) on Wiley Online Library for rules of use; OA articles are governed by the applicable Creative Commons License

4.2 | Chemical Anisotropy

This type of anisotropy arises from direction-dependent chemical characteristics on the surface. A common example includes surfaces with wettability gradient patterns, comprising regions of varying hydrophobicity and hydrophilicity. On such surfaces, unidirectional droplet motion can occur as droplets naturally migrate toward areas with higher wettability. Janus structures, which exhibit dual wetting properties on different sides of a membrane, also represent a prominent example of this type of anisotropy. Various fabrication techniques have been developed to engineer these chemically anisotropic wetting surfaces.

4.2.1 | Photolithography and Etching

Microscale hydrophilic-hydrophobic patterns/structures can be easily fabricated using a one-step photolithography method. Wu et al. used this technique to create highly adherent wettability patterns on substrate-independent superhydrophobic surfaces composed of trimethoxyoctadecylsilane (TMOS)-modified titanium dioxide (TiO_2) coatings [125]. By exposing these coatings to UV light through a patterned photomask, three unidirectional channel-shaped gradient wettability patterns were formed. UV exposure selectively transformed the exposed regions into superhydrophilic areas, while the unexposed parts retained their superhydrophobic properties.

Similarly, wedge-shaped wettability gradient structures were fabricated using photolithography and SiO_2 deposition on hydrophobic cyclo olefin polymer (COP) substrates [126]. Droplets placed on the hydrophobic COP regions migrated toward the hydrophilic SiO_2 regions, demonstrating effective transport of droplets.

However, surfaces fabricated solely through photolithography exhibit limited droplet transport distances and low speeds, primarily due to weak wettability gradients. To address this limitation and enable long-range droplet transportation, photolithography can be combined with etching. For instance, Liu et al. developed gradient structures featuring hydrophilic SiO_2 stripes with varying densities interspersed with hydrophobically modified nanowires by integrating photolithography and etching techniques [127]. These gradient surfaces facilitated the transportation of droplets over extended distances (up to 37.5 mm) from superhydrophobic nanowire regions to hydrophilic SiO_2 stripe-patterned areas.

4.2.2 | Selective Depositions

Patterned gradient wetting surfaces can be created by selectively depositing specific materials onto target surfaces. For instance, superhydrophilic-superhydrophobic patterned surface structures have been fabricated using a pulsed laser deposition technique [128]. The process begins by spraying the substrate with silica-PDMS aerogel to achieve a superhydrophobic base.

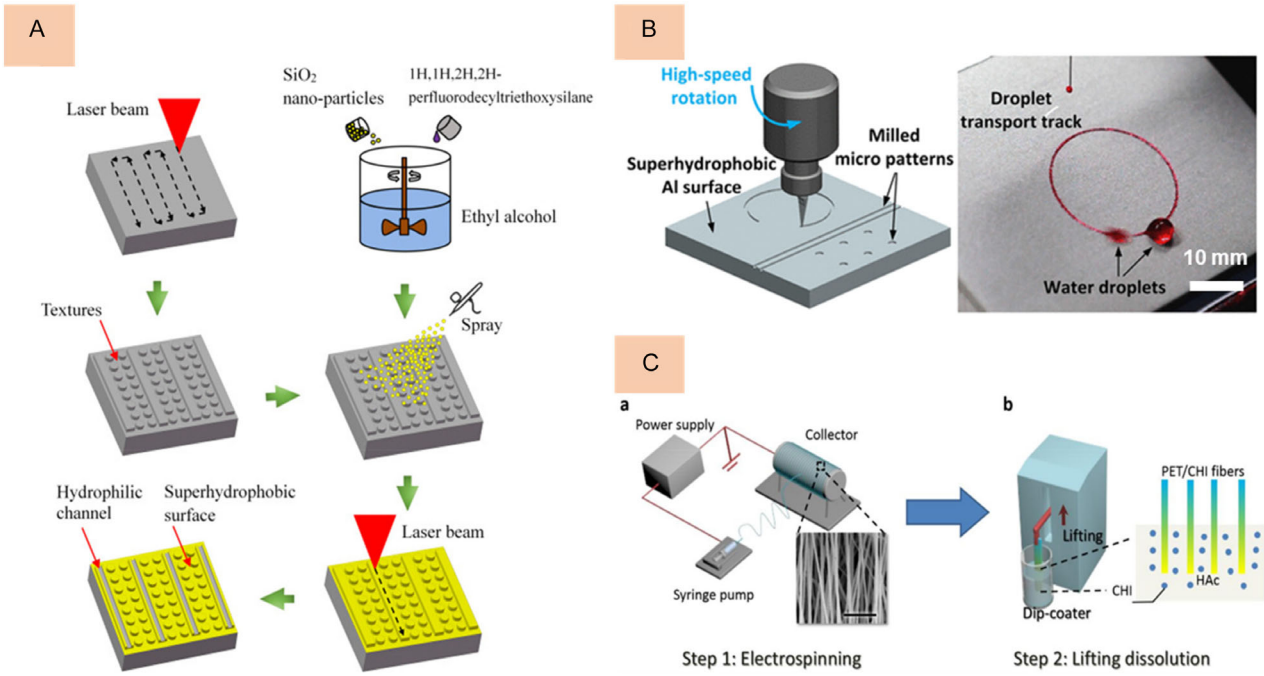


FIGURE 13 | Schematics illustrating examples of available fabrication methods for creating surfaces with wettability contrast property. (A) Fabrication process of the superhydrophobic/hydrophilic hybrid textured surface. First, laser micromachining is used to fabricate microtextures on an aluminum alloy (Al-Zn-Mg-Cu) surface by controlling the scanning path. Second, SiO_2 nanoparticles, 1H, 1H,2H, 2H-perfluorodecyltriethoxysilane and ethyl alcohol are mixed and sprayed on prefabricated textured surface structure. After drying at room temperature, the micro-nano fractal superhydrophobic surface is prepared. Third, laser ablating is used to create hydrophilic microchannels on the convex stripes. Reproduced with permission from [99], Copyright 2021, Elsevier. (B) Schematic illustration of the fabrication process of hydrophilic designs (micro dots, line, and circle grooves) on a superhydrophobic surface using the micromilling technique. Reproduced with permission from [130], Copyright 2016, American Chemical Society (ACS). (C) Schematic view of the fabrication process of a WG-aligned PET/CHI fibrous surface. (a) Electrospinning machine with a high-speed-rotated collector for preparing aligned PET/CHI fiber. (b) Lifting dissolution strategy for CHI-composition gradient formation. Reproduced with permission from [131], Copyright 2015, Wiley-VCH.

26884062, 2026, 2, Downloaded from https://onlinelibrary.wiley.com/doi/10.1002/sstr.202500492 by Scholarly Resource Services, Wiley Online Library on [04/11/2026]. See the Terms and Conditions (https://onlinelibrary.wiley.com/terms-and-conditions) on Wiley Online Library for rules of use; OA articles are governed by the applicable Creative Commons License

Subsequently, superhydrophilic platinum nanoparticles are deposited onto the superhydrophobic surface through a patterned stainless-steel mask. The extent of nanoparticle-coated areas can be controlled by adjusting the parameters of the mask.

4.2.3 | Laser Micromachining

Laser-based techniques are widely recognized for their fast, precise, and efficient capabilities in fabricating wettability contrast surfaces [129]. For instance, Zhang et al. successfully fabricated a microscale fractal superhydrophobic surface with hydrophilic patterned microchannels using a direct laser writing method. The detailed fabrication process is illustrated in Figure 13A [99].

Furthermore, laser technology itself has a decisive role in controlling liquid transport performance. A recent study by Zoudani et al. showcased the fabrication of a microchannel structure on a chemically modified prelaser textured hydrophobic square background on silicon wafer [132]. The fabricated pattern displayed contrasting wetting properties: the prelaser-machined square background retained hydrophobic characteristics, while the laser-textured microchannel exhibited efficient wicking behavior. The study revealed that the wicking flow rate is strongly influenced by the specific roughness features generated by the laser, emphasizing the importance of laser-induced surface modifications in optimizing liquid transport performance.

4.2.4 | Micromilling Method

Micromilling method has also been demonstrated as a fast, efficient, and flexible technique for preparing surfaces with wettability contrasts. This approach enables the creation of various linear patterns on different substrates through its mechanical material removal mechanism [130]. For instance, Yang et al. utilized micromilling to fabricate hydrophilic designs, including microdots, line grooves, and circular grooves, on a superhydrophobic surface [130], as illustrated in Figure 13B.

4.2.5 | Other Methods

In addition to the methods mentioned earlier, other techniques can be used to prepare surfaces with wettability contrasts. Zhang et al. reported the fabrication of a wettability gradient-aligned polyester (PET)/chitosan (CHI) fibrous surface [131].

TABLE 2 | Summary of the studies dedicated to the fabrication of anisotropic surfaces with wettability contrasts.

Structural feature	Control avenue	Fabrication method	Advantages
Micro- and nano-fractal superhydrophobic surfaces patterned with micro hydrophilic stripe-type channels [99]	Affinity and prewetting effect of hydrophilic channels	Laser direct writing method	Droplet sliding along different shapes (straight, curved or S-shaped) of designed pathways. These moving actions can be continued even if the surface gets completely inverted.
Wettability-patterned gradient on substrate-Independent trimethoxyoctadecylsilane modified titanium dioxide (TiO_2)-based coated superhydrophobic surfaces [125]	Passive droplet transportation resulted from surface wettability gradient patterns	Photolithography	Realization of droplet metering, merging or reaction and rapid transportation with no need for any external stimuli, or additives. Potential of using as a pump-free microfluidic device for droplet merging with accurate volume for specific interactions
Desert beetle-inspired superhydrophilic/superhydrophobic patterned surfaces fabricated on the silica PDMS- coated superhydrophobic surfaces [128]	Passive droplet transportation resulted from Surface wettability gradient	The pulsed laser deposition (PLD)	Great capability of water-harvesting, suitable for both night-time humid desert areas and high-level steam, e.g., thermal desalination plants and waste steam in steel plants and steam engines. Efficient fabrication technique for superwettable patterned surfaces for large-scale water harvesting application, making it a relief to growing global water crisis.
Superhydrophobic Al alloy surface with hydrophilic milled patterns [130]	Surface wettability gradient results in passive droplet transportation on micromilled structures	Micromilling technology	Micromilling technology is a direct, environmental-friendly, easy-to operate technique based on its mechanical material-removal capability. Through controlling the size of the milled structures, the adhesion force towards droplet is regulated.

26884062, 2026, 2, Downloaded from https://onlinelibrary.wiley.com/doi/10.1002/sstr.202500492 by Scholarly Resource Services, Wiley Online Library on [04/11/2026]. See the Terms and Conditions (https://onlinelibrary.wiley.com/terms-and-conditions) on Wiley Online Library for rules of use; OA articles are governed by the applicable Creative Commons License

The surface structure was created by combining electrospinning and lifting-dissolution techniques, with wettability controlled by adjusting PET-CHI composition, acetic acid concentration, and lifting rate. The fabrication process is illustrated in Figure 13C.

Lee et al. proposed a straightforward and mendable approach for generating various hydrophilic patterns on superhydrophobic surfaces [133]. This process involved creating a uniform superhydrophobic layer using atmospheric radio frequency (RF) plasma and selectively printing hydrophilic patterns with polar alcohols using the electro-hydrodynamic (EHD) jet printing technique.

Additionally, Liu et al. introduced a versatile electro-spraying method to fabricate a patterned PDMS/PMMA coating with asymmetrical wettability [134]. These tunable superwetting patterns offer significant functional versatility. For instance, superhydrophobic fabric serves as an efficient separation filter with cycling capabilities. The wettability differences in these patterned surfaces enable control over the successive motions of droplets.

Table 2 summarizes the studies discussed in Section 4 regarding the fabrication of surfaces with wettability contrasts.

4.2.6 | Fabrication Methods for Janus Micropillars

Janus surfaces, defined by their asymmetric molecular modifications with distinct surface energies, demonstrate remarkable anisotropic wettability and are highly effective for droplet manipulation applications. The directional movement of droplets on Janus heterogeneous surfaces is driven by surface tension differences, causing transportation toward regions of higher surface energy [5].

For instance, a thermally responsive Janus Si micropillar array with anisotropic wettability was fabricated using thermal-responsive poly(N-isopropylacrylamide) (PNIPAM) brushes coated onto a Janus Si pillar array [58]. These surfaces switch between isotropic and anisotropic wetting properties depending on the PNIPAM molecule's transition between hydrophilic and hydrophobic states at temperatures below or above its lower critical solution temperature (LCST). The elliptical morphology of the micropillar structure enhanced anisotropic wettability, and the fabrication process is depicted in Figure 14A. The final surface featured Janus-modified Si micropillars coated on one side with PNIPAM brushes and on the other with a mercaptohexadecanoic acid (MHA) layer.

In another study, researchers fabricated a multi-bioinspired Janus structure that incorporated asymmetric features inspired

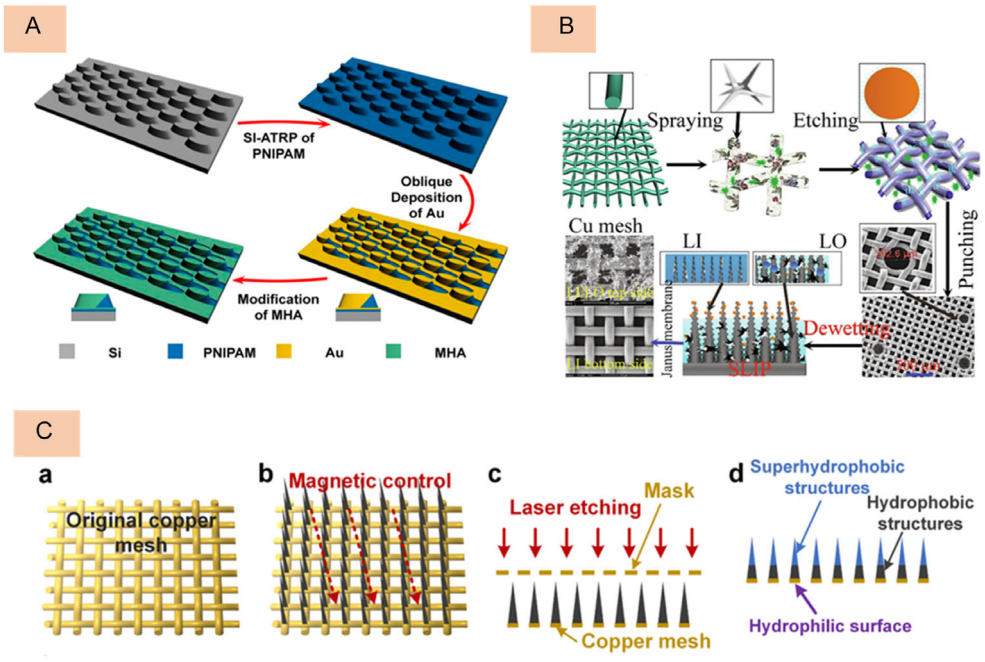


FIGURE 14 | Examples of available fabrication methods for creating Janus surfaces. (A) Preparation mechanism of PNIPAM/MHA Janus Si micropillar array. The Si micropillar structure with elliptical geometry was first fabricated by the etching method. Micropillar array surface modification was performed with a layer of poly(N-isopropylacrylamide) (PNIPAM) brush. After that, the oblique Au deposition process was done. After the deposition of Au layer, surface modification was performed via self-assembled monolayer of hydrophilic 16-mercaptohexadecanoic acid (MHA) molecules. Reproduced with permission from [58], Copyright 2015, American Chemical Society (ACS). (B) Preparation procedure of the multibioinspired hybrid Janus membrane. First, ZnO-tetrapod layer was sputtered onto a pristine smooth Cu grid, Cu(OH)2 nanofibers were created from the Cu mesh surface, then passed through the ZnO-tetrapod network through etching, forming an interpenetrating lyophobic/lyophilic Janus membrane. Dewetting was performed to prepare multiple superwettable Janus membranes. Reproduced with permission from [135], Copyright 2021, Elsevier. (C) (a–d) Fabrication process of the Janus membrane with wettability gradient conical arrays. First, the oxide on the copper mesh surface was removed by ultrasonic cleaning. After natural drying, the conical array structure was formed by a modified particle-assisted molding (MPAM) method. Finally, wettability gradients on micropillars were created through laser etching of the conical array structure under a copper mesh mask. Reproduced with permission from [136], Copyright 2021, American Chemical Society (ACS).

26884062, 2026, 2, Downloaded from https://onlinelibrary.wiley.com/doi/10.1002/sstr.202500492 by Scholarly Resource Services, Wiley Online Library on [04/11/2026]. See the Terms and Conditions (https://onlinelibrary.wiley.com/terms-and-conditions) on Wiley Online Library for rules of use; OA articles are governed by the applicable Creative Commons License

by the cactus spines, lyophilic/lyophobic micropatterns of beetle backs, edge-shaped microgrooves of Nepenthes peristome, and aquatic plant pumping strategies [135]. The Janus membrane, combining spraying and etching fabrication methods, featured an interpenetrating structure with heterogeneous wetting properties, as illustrated in Figure 14B. The structure included $Cu(OH)_2$ nanofibers and ZnO-tetrapods with lyophilic and lyophobic regions, achieved by tuning the deposition of low-energy silicone oil during a dewetting procedure. This design enabled droplets to converge at micropores, moving by capillary forces and slippery features provided by the Janus membrane.

Additionally, a Janus membrane with wettability gradient conical arrays was fabricated using magnetic control and laser etching on a copper mesh [136], as shown in Figure 14C. The process involved clearing surface oxides from the copper mesh, followed by forming conical arrays through a modified particle-assisted molding (MPAM) method. Laser etching was then used to create wettability gradient regions. The hydrophilic copper mesh surface exhibited hydrophobic behavior in masked areas and superhydrophobic properties at the apexes of conical micropillars above the mask.

Table 3 provides a concise summary of the studies discussed in this section.

5 | Applications of Unidirectional Wetting Surfaces

Applications currently focus mainly on three main sectors: (1) Organ-on-chip channel, (2) through-thickness membrane, and (3) surface designs.

Most of the fluid flows in the human body, including blood circulation, the lymphatic system, the urinary system, and the digestive system, are unidirectional [137–140]. These systems contain active or passive valve-like structures to produce and maintain the unidirectional flow. Thus, organ-on-chip designs specifically utilize unidirectional flows to more accurately mimic microphysiological systems [52, 141–143].

Although a significant number of research studies have been focused on the development of unidirectional wetting surfaces, most of the developed devices remain restricted to research settings. These surfaces or structures are predominantly found in microfluidic devices for passive flow control [144]. These surfaces can replace the valves in microfluidic devices, reducing the mechanical complexity and improving the durability. They utilize special surface structures that create different fluid resistances in different directions, making flow in one direction easier than in the other [145]. For example, Tesla valves are a unique structural design that is commonly seen in microfluidic devices as a passive valve. However, these passive devices cannot fully restrict the flow in the opposite direction.

Membranes with unidirectional fluid transport ability are also unique devices based on wettability gradient across the membrane, which shows potential for several practical applications, such as unidirectional drug delivery [146]. Moisture-wicking fabrics are a commercially available application of unidirectional wetting membranes, utilizing capillary action and the wettability gradient between two fabric layers. The inner layer of these fabrics is hydrophilic to absorb and transport sweat unidirectionally from the skin to the outer layer, which in turn promotes evaporation, keeping the skin surface dry [147]. Additionally, Janus fabrics with differing wetting properties on each side represent a new approach to moisture-wicking fabric design [148, 149]. These fabrics feature an array of conical microchannels with a larger diameter on the skin-contacting surface, inspired by the shorebird's beak mechanism, which facilitates directional liquid transport away from the skin [150]. Dong et al. proposed the use of a similar film to enable self-sweat pumping, enhancing the comfort of wearable sensors for extended use [151]. They fabricated this film by stacking several layers of fabrics with different porosities to induce a wettability gradient. Also, where direct contact with skin is not required, biosensors can be mounted on the fabric, as the fabric effectively transports sweat from the skin to the sensor.

Janus wound dressings are a novel application of unidirectional wetting fabrics [152, 153]. These dressings show hydrophobic

TABLE 3 | Summary of the studies dedicated to fabrication of anisotropic surfaces with Janus structures for unidirectional liquid transport.

Structural feature	Control avenue	Fabrication method	Advantages
Janus micropillar array (MPA) with wettability-switchable polymer brush on one side and hydrophilic self-assembled monolayer on the other [58]	External heat source	Etching and deposition methods	Ability of liquid droplet manipulation, potency of using as a smart thermo-valve in microfluidic system
Multibioinspired Janus membrane with heterogeneous wetting and interpenetrating structure [135]	Surface energy gradient and Laplace pressure difference resulted from hydrophobic/hydrophilic patterns	Spraying and etching method	Ability to recycle the fog droplets absorption, growth, directional pumping and penetration.
Janus membrane with conical arrays of the wettability gradient [136]	Passive droplet transportation assisted by wettability gradient from the surface tension of the droplets and the capillary force	Magnetic control and laser etching	Enhanced fog collection rate of about 7.05 $g/cm^2/h$.

26884062, 2026, 2, Downloaded from https://onlinelibrary.wiley.com/doi/10.1002/sstr.202500492 by Scholarly Resource Services, Wiley Online Library on [04/11/2026]. See the Terms and Conditions (https://onlinelibrary.wiley.com/terms-and-conditions) on Wiley Online Library for rules of use; OA articles are governed by the applicable Creative Commons License

properties on the outside surface, which will prevent the absorption of liquids and the entrance of any contaminants. The hydrophilic inside layer absorbs any exudates from the wound and pumps them to the outside through the wettability gradient [154]. This technique can reduce the risk of infections in wounds while maintaining the dryness and breathability of the dressing. Lin et al. showed that these Janus dressings can improve the wound healing rate from 87.65% to 100% while showing the ability to unidirectionally transport loaded drugs to the wound. Similarly, Cheng et al. propose the use of Janus-like fabrics for the fabrication of face masks, which will prevent the droplets from wetting the outside surface, which could potentially contain any infectious materials [155].

Water/oil separation is another application of Janus substrates with a wettability gradient. These membranes have two sides, such that one side is hydrophilic/oleophobic while the other is hydrophobic/oleophilic. Thus, one side of the substrates can selectively absorb and drive one liquid with particular wettability properties in one direction, separating it from the other [156, 157]. Similar membranes are also used in solar absorbers for saltwater desalination [158]. These substrates effectively transport water from the underlying reservoir to the heated surface, promoting evaporation [159].

Inspired by the natural fog collection mechanism of the desert beetle and cactus spines, unidirectional surfaces have been used on fog collection devices [160]. These surfaces provide hydrophilic regions that promote droplet condensation through a low-energy barrier, and condensed droplets are transported unidirectionally to hydrophobic areas for collection [147]. Ding et al. showed the utilization of a Janus membrane made with modified natural wood to capture fog and transport them into a reservoir. They could capture 2.92 kgm^{-2} in an hour from saturated fog compared to only 1.16 kgm^{-2} water condensation with native wood without Janus modification.

Leveraging the unique morphological elements and material properties, the generated designs can be tailored to specific applications. For instance, biomimetic ribbon-like structures composed of liquid crystal elastomers (LCEs) were engineered for water collection [161]. By tuning the director orientation within the LCEs, diverse morphological evolutions, including bending, twisting, and spiraling, were achieved. Under external stimuli, the twisting configuration not only facilitated efficient water droplet transport but also exhibited enhanced resistance to wind and rainfall.

These surfaces, with their unique capability for directional water transport, can also be extended to liquid–liquid chemical reactions. On such micropatterned substrates, directional droplet transport enables controlled movement, coalescence, and subsequent reactions between droplets. This property allows droplets to freely migrate, merge, and react in a programmable manner, thereby offering a powerful strategy for conducting chemical microreactions. Such an approach holds great potential for the development of lab-on-a-chip platforms, where directional droplet manipulation can facilitate efficient reaction control and downstream analytical processes [162].

Surfaces with unidirectional wetting properties are also evident as a drag reduction mechanism of swimming suits and aquatic surfaces. Especially sharkskin-like riblet patterns can reduce the directional fluid drag by controlling the vortices on the surfaces, reducing the momentum transfer and shear stress [163, 164].

6 | Challenges and Limitations

Designing and developing anisotropic surfaces with unidirectional wetting properties remains a challenging yet rapidly advancing area of research. Despite numerous breakthroughs, achieving an ideal surface that meets all key design criteria, such as fast response time, precise directional control, high durability, low energy consumption, and scalable fabrication, remains elusive. These criteria, discussed throughout this review, are often interdependent and subject to trade-offs. For instance, increasing structural complexity may enhance directional precision but compromise scalability or fabrication cost. Therefore, the successful implementation of these surfaces requires a holistic approach that addresses both fundamental material limitations and practical engineering constraints. This section highlights the most pressing technical and conceptual challenges that must be overcome to advance the field toward real-world applications.

Various interrelated factors must be considered when designing anisotropic surfaces with unidirectional wetting properties. These include selecting appropriate materials, choosing fabrication methods, and determining parameters that govern liquid behavior, such as droplet size, viscosity, surface energy gradients, and responsiveness to external stimuli. Often, enhancing one functional aspect, such as directional precision or responsiveness, comes at the cost of others, including scalability, mechanical robustness, or fabrication complexity. As a result, designing an optimal surface requires a careful balancing of trade-offs, guided by the specific requirements of the intended application. The following discussion highlights the key technical and conceptual challenges that continue to limit the widespread adoption and performance of these surfaces.

The versatility, cost-effectiveness, equipment accessibility, and flexibility of the fabrication method are critical in determining the feasibility and scalability of unidirectional wetting surface designs. Equally important is the careful selection of target materials, which directly influence the surface's chemical compatibility, wettability range, and long-term performance. For example, PDMS is widely used due to its low cost, optical transparency, biocompatibility, and ease of replication through molding. These features make it ideal for applications such as microfluidics and lab-on-a-chip systems. However, PDMS's inherent hydrophobicity and chemical inertness can hinder applications in cell biology and make surface functionalization for anisotropic wettability difficult. It is also known to absorb small hydrophobic molecules, potentially interfering with bioanalytical assays [165].

Other materials offer alternative benefits and limitations. PTFE, for instance, exhibits excellent chemical resistance and a low surface energy, making it suitable for robust, passive anisotropic wetting surfaces; however, its low adhesion and poor processability limit high-resolution patterning. Metallic substrates such as aluminum and copper are often used in laser-based fabrication due to their mechanical rigidity and thermal conductivity, yet they typically require additional surface modifications to achieve

26884062, 2026, 2, Downloaded from https://onlinelibrary.wiley.com/doi/10.1002/sstr.202500492 by Scholarly Resource Services, Wiley Online Library on [04/11/2026]. See the Terms and Conditions (https://onlinelibrary.wiley.com/terms-and-conditions) on Wiley Online Library for rules of use; OA articles are governed by the applicable Creative Commons License

the necessary wetting contrasts. Thus, material choice must be tailored to the specific application, fabrication method, and target performance metrics.

As previously elaborated, from the perspective of directional fluid transport, anisotropic wetting surfaces function through two primary mechanisms: active and passive. Each mechanism has distinct advantages and limitations. While active approaches allow for dynamic control, they are not without drawbacks. For instance, using heat for droplet manipulation can lead to unintended droplet evaporation [42], undermining the goal of lossless droplet transport. Similarly, external fields can alter droplet composition, making them unsuitable for biological applications. Additionally, the reliance on external equipment, increased costs, and dependency on external fields throughout the whole process reduce the practicality of active mechanisms in certain scenarios.

In contrast, passive mechanisms achieve droplet transportation solely through the inherent properties of wetting surfaces, eliminating the need for external stimuli. However, passive approaches face challenges such as slower droplet motion, limited directional control, and reduced transport distances due to energy loss on wettability-patterned surfaces [166].

To move toward optimal designs, a balanced evaluation of these factors is required to identify the most suitable platform that effectively meets primary requirements. A deeper examination of these structures reveals that their wettability, whether superhydrophobic for droplet transport or superhydrophilic for continuous fluid transport, can be achieved through two main strategies.

The first strategy involves engineering microstructures, a physical approach that creates specific surface morphologies to induce desired wetting properties. However, this method presents challenges, such as the availability of suitable fabrication equipment, the feasibility of the methods, and the precision required for producing microscale structures.

The second strategy relies on chemical modifications, where surfaces are coated with chemical layers to alter their surface chemistry and achieve specific wettability. While this approach is relatively simpler, it comes with limitations, including the degradation of coatings under environmental conditions. Stability, durability, and biosafety are critical concerns, particularly for applications in healthcare and biomedical fields.

Moreover, while chemical modifications are straightforward, microstructured surfaces offer better maneuverability over liquid behavior. They provide superior manipulation of droplet morphology, transport rate, and movement direction. Such characteristics are difficult to achieve with chemical coatings alone.

Despite significant advancements in experimental techniques, the theoretical modeling and numerical simulation of anisotropic wetting remain in the early stages of development [167]. While thermodynamic analyses have provided foundational insights, they often fall short in capturing the complexities of dynamic wetting behaviors on structured surfaces. Numerical methods, such as the Lattice Boltzmann method and Surface Evolver simulations, have been used to study droplet behavior on anisotropic surfaces. However, existing models often struggle to accurately capture complex phenomena such as contact line dynamics, wetting hysteresis, and energy dissipation during droplet impact. For instance, Jiang et al. conducted an experimental study on the dynamic characteristics and energy variation of droplets impacting quartz surfaces, revealing four distinct stages of droplet behavior and highlighting the intricate energy transformations involved [168]. However, translating such detailed experimental observations into predictive models is challenging. The development of robust computational frameworks that can simulate these complex interactions is essential for advancing the design and optimization of anisotropic wetting surfaces.

7 | Conclusions and Future Directions

The development of micropatterned surfaces with unidirectional wetting properties has significantly improved our ability to control fluid dynamics in various applications. These surfaces have shown great promise in applications such as microfluidics, water harvesting, and biomedicine. However, some intrinsic challenges remain, mainly related to scalability, reproducibility, and durability under realistic conditions.

A promising outlook for future research lies in integrating these surfaces with microfluidic systems, using their synergistic properties to reveal new possibilities. Combining the precision of microfluidics with the advanced liquid manipulation capabilities of unidirectional wetting surfaces makes it possible to create flexible and efficient platforms for liquid transportation, diagnostic applications, and chemical processing.

Second, the new discipline related to hydrodynamic metamaterials offers vast prospects for creating novel, next-generation unidirectional wetting surfaces. Artificially synthesized materials possess certain features that effectively control fluid dynamics through purposefully engineered anisotropic properties, possibly evading various complexities in surface engineering. Hydrodynamic metamaterials can provide functionalities such as cloaking, concentrating, or guiding flows in highly controlled manners. Integration with unidirectional surfaces may ultimately lead to adaptive, multifunctional platforms that can dynamically respond to environmental stimuli or application-specific requirements.

Finally, future progress will also depend on advances in theoretical modeling and numerical simulations, which can provide deeper insights into the underlying mechanisms of unidirectional fluid transport. The integration of artificial intelligence (AI) and machine learning (ML) will further accelerate this field by enabling the optimization of micro/nanostructures for specific flow regimes. Such predictive design frameworks hold great promise for rapidly identifying novel geometries and unlocking unique functionalities, thereby expanding the potential applications of micropatterned surfaces in fluid manipulation.

Further work should focus on developing scalable processing methods and durable materials that can maintain their one-sided

26884062, 2026, 2, Downloaded from https://onlinelibrary.wiley.com/doi/10.1002/sstr.202500492 by Scholarly Resource Services, Wiley Online Library on [04/11/2026]. See the Terms and Conditions (https://onlinelibrary.wiley.com/terms-and-conditions) on Wiley Online Library for rules of use; OA articles are governed by the applicable Creative Commons License

wetting features over a spectrum of operating environments. Interdisciplinary contributions from the material science, fluid mechanics, and bioengineering communities are going to be imperative to meet the challenges head-on and also to enlarge the possible fields of application for such surfaces.

More studies are required to rigorously establish the relative merits of different wetting-imposition strategies, chemical gradients versus purely physical structuring, particularly from the perspectives of scalability, translational potential, and application-specific performance. Systematic comparisons should evaluate not only directional transport efficiency but also manufacturability at scale, material cost and availability, long-term durability, and compatibility with downstream commercial processes. Such evidence will be critical to determine which approach is most practical for translating micropatterned surfaces from benchtop demonstrations to real-world devices.

In summary, while the search for optimal designs of unidirectional wetting surfaces is an ongoing activity, integrating such designs into microfluidic systems and exploring configurations inspired by metamaterials presents exciting opportunities. Such advances will reveal new directions in liquid transport, providing innovative solutions for sustainable water management, enhanced diagnostic methods, and more.

Author Contributions

Elham Lori Zoudani: investigation (lead), methodology (lead), software (lead), validation (equal), visualization (lead), writing – original draft (lead). **Prabuddha De Saram**: investigation (equal), methodology (equal), visualization (supporting), writing – original draft (supporting). **Stefanie Feih**: formal analysis (supporting), investigation (supporting), methodology (supporting), validation (supporting) writing – review and editing (equal). **Hoang Huy Vu**: investigation (supporting), methodology (supporting), visualization (supporting), writing – original draft (supporting). **Nam-Trung Nguyen**: formal analysis (equal), funding acquisition (equal), investigation (equal), methodology (equal), project administration (equal), resources (equal), supervision (equal), writing – review and editing (equal). **Navid Kashaninejad**: conceptualization (lead), data curation (equal), formal analysis (lead), funding acquisition (lead), investigation (equal), methodology (equal), project administration (lead), resources (lead), supervision (lead), validation (equal), visualization (equal), writing – original draft (equal), writing – review and editing (equal).

Acknowledgements

N.K. acknowledges funding support from the Australian Research Council (ARC) Discovery Early Career Research Award (DECRA) DE220100205. N.-T.N. acknowledges funding support from the Australian Research Council (ARC) through the Australian Laureate Fellowship (FL230100023).

Open access publishing facilitated by Griffith University, as part of the Wiley - Griffith University agreement via the Council of Australian University Librarians.

Conflicts of Interest

The authors declare no conflicts of interest.

Data Availability Statement

The data that support the findings of this study are available from the corresponding author upon reasonable request.

References

1. D. Xia, L. M. Johnson, and G. P. López, "Anisotropic Wetting Surfaces with One-Dimesional and Directional Structures: Fabrication Approaches, Wetting Properties and Potential Applications," *Advanced Materials* 24, no. 10 (2012): 1287–1302.

2. E. Pierce, F. Carmona, and A. Amirfazli, "*Understanding of Sliding and Contact Angle Results in Tilted Plate Experiments." Colloids and Surfaces A: Physicochemical and Engineering Aspects*, 323, no. 1–3 (2008): 73–82.

3. J. Macko, N. Podrojkova, R. Oriňaková, and A. Oriňak, "New Insights into Hydrophobicity at Nanostructured Surfaces: Experiments and Computational Models," *Nanomaterials and Nanotechnology* 12 (2022): 18479804211062316.

4. N. Kashaninejad, N.-T. Nguyen, and W. K. Chan, "Eccentricity Effects of Microhole Arrays on Drag Reduction Efficiency of Microchannels with a Hydrophobic Wall," *Physics of Fluids* 24, no. 11 (2012).

5. P. Ge, S. Wang, J. Zhang, and B. Yang, "Micro-/Nanostructures Meet Anisotropic Wetting: From Preparation Methods to Applications," *Materials Horizons* 7, no. 10 (2020): 2566–2595.

6. N. Kashaninejad, N.-T. Nguyen, and W. K. Chan, "The Three-Phase Contact Line Shape and Eccentricity Effect of Anisotropic Wetting on Hydrophobic Surfaces," *Soft Matter* 9, no. 2 (2013): 527–535.

7. Y.-E. Lee, D.-K. Lee, and Y. H. Cho, "Fabrication of Anisotropic Wetting Surface with Asymmetric Structures Using Geometrical Similarity and Capillary Force," *Micro and Nano Systems Letters* 7 (2019): 1–7.

8. M. Li, C. Li, B. R. Blackman, and S. Eduardo, "Mimicking Nature to Control Bio-Material Surface Wetting and Adhesion," *International Materials Reviews* 67, no. 6 (2022): 658–681.

9. E. L. Zoudani, N.-T. Nguyen, and N. Kashaninejad, "Engineering Wettability Transitions on Laser-Textured Shark Skin-Inspired Surfaces via Chemical Post-Processing Techniques," *Micromachines* 15, no. 12 (2024): 1442.

10. N. Kashaninejad, W. K. Chan, and N.-T. Nguyen, "Eccentricity Effect of Micropatterned Surface on Contact Angle," *Langmuir* 28, no. 10 (2012): 4793–4799.

11. R. Malinowski, I. P. Parkin, and G. Volpe, "Advances towards Programmable Droplet Transport on Solid Surfaces and Its Applications," *Chemical Society Reviews* 49, no. 22 (2020): 7879–7892.

12. N. Kashaninejad, M. J. A. Shiddiky, and N. T. Nguyen, "Advances in Microfluidics-Based Assisted Reproductive Technology: From Sperm Sorter to Reproductive System-on-a-Chip," *Advanced Biosystems* 2, no. 3 (2018): 1700197.

13. Y. Zhang, Y. Gan, L. Zhang, Y. Guo, Y. Wang, Z. Wang, X. Liu, P. Zhang, T. Ran, and L. Jiang, "*Controllable Directional Liquid Transport in Open Channel." Advanced Materials Interfaces*, 9, no. 14 (2022): 2102547.

14. T. Xu, Y. Lin, M. Zhang, W. Shi, and Y. Zheng, "High-Efficiency Fog Collector: Water Unidirectional Transport on Heterogeneous rough Conical Wires," *ACS Nano* 10, no. 12 (2016): 10681–10688.

15. M. He, Q. Zhang, X. Zeng, D. Cui, J. Chen, H. Li, J. Wang, and Y. Song, "Hierarchical Porous Surface for Efficiently Controlling Microdroplets' Self-Removal," *Advanced Materials* 16, no. 25 (2013): 2291–2295.

16. S. Nishimoto and B. Bhushan, "Bioinspired Self-Cleaning Surfaces with Superhydrophobicity, Superoleophobicity, and Superhydrophilicity," *RSC Advances* 3, no. 3 (2013): 671–690.

26884062, 2026, 2, Downloaded from https://onlinelibrary.wiley.com/doi/10.1002/sstr.202500492 by Scholarly Resource Services, Wiley Online Library on [04/11/2026]. See the Terms and Conditions (https://onlinelibrary.wiley.com/terms-and-conditions) on Wiley Online Library for rules of use; OA articles are governed by the applicable Creative Commons License

17. L. Zhang, G. Liu, H. Chen, X. Liu, T. Ran, Y. Zhang, Y. Gan, and D. Zhang, "Bioinspired Unidirectional Liquid Transport Micro-Nano Structures: A Review," *Journal of Bionic Engineering* 18 (2021): 1–29.

18. N. A. Malvadkar, M. J. Hancock, K. Sekeroglu, W. J. Dressick, and M. C. Demirel, "An Engineered Anisotropic Nanofilm with Unidirectional Wetting Properties," *Nature Materials* 9, no. 12 (2010): 1023–1028.

19. K. S. Khalil, S. R. Mahmoudi, N. Abu-Dheir, and K. K. Varanasi, "Active Surfaces: Ferrofluid-Impregnated Surfaces for Active Manipulation of Droplets," *Applied Physics Letters* 105 (2014): 4.

20. S. Lowrey, K. Misiiuk, R. Blaikie, and A. Sommers, "Survey of Micro/Nanofabricated Chemical, Topographical, and Compound Passive Wetting Gradient Surfaces," *Langmuir* 38, no. 2 (2022): 605–619.

21. M. Soltani and K. Golovin, "Lossless, Passive Transportation of Low Surface Tension Liquids Induced by Patterned Omniphobic Liquidlike Polymer Brushes," *Advanced Functional Materials* 32, no. 1 (2022): 2107465.

22. H. Bai, T. Zhao, and M. Cao, "Interfacial Fluid Manipulation with Bioinspired Strategies: Special Wettability and Asymmetric Structures," *Chemical Society Reviews* 54, no. 6 (2025): 1733-1784.

23. E. Lori Zoudani, N. T. Nguyen, and N. Kashaninejad, "Microneedle Optimization: Toward Enhancing Microneedle's Functionality and Breaking the Traditions," *Small Structures* 5, no. 12 (2024): 2400121.

24. W. Zhang, J. Xu, and T. Yu, "Dynamic Behaviors of Bio-Inspired Structures: Design, Mechanisms, and Models," *Engineering Structures* 265 (2022): 114490.

25. S. Wei and T. K. Ghosh, "Bioinspired Structures for Soft Actuators," *Advanced Materials Technologies* 7, no. 10 (2022): 2101521.

26. T. Kong, G. Luo, Y. Zhao, and Z. Liu, "Bioinspired Superwettability Micro/Nanoarchitectures:Fabrications and Applications," *Advanced Functional Materials* 29, no. 11 (2019): 1808012.

27. L. Feng, S. Li, Y. Li, H. Li, L. Zhang, J. Zhai, Y. Song, B. Liu, L. Jiang, and D. Zhu, "Super-Hydrophobic Surfaces: From Natural to Artificial," *Advanced Materials* 14, no. 24 (2002): 1857–1860.

28. S. G. Lee, H. S. Lim, D. Y. Lee, D. Kwak, and K. Cho, "Tunable Anisotropic Wettability of Rice Leaf-Like Wavy Surfaces," *Advanced Functional Materials* 23, no. 5 (2013): 547–553.

29. Y. Cai, L. Lin, Z. Xue, M. Liu, S. Wang, and L. Jiang, "Filefish-Inspired Surface Design for Anisotropic Underwater Oleophobicity," *Advanced Functional Materials* 24, no. 6 (2014): 809–816.

30. Z. Wang, Y. Lu, S. Huang, S. Yin, and F. Chen, "Bamboo-Joint-Like Platforms for Fast, Long-Distance, Directional, and Spontaneous Transport of Fluids," *Biomicrofluidics* 14 (2020): 3.

31. H. Wu, R. Zhang, Y. Sun, D. Lin, Z. Sun, W. Pan, and P. Downs, "Biomimetic Nanofiber Patterns with Controlled Wettability," *Soft Matter* 4, no. 12 (2008): 2429–2433.

32. Y. Zheng, X. Gao, and L. Jiang, "Directional Adhesion of Superhydrophobic Butterfly Wings," *Soft Matter* 3, no. 2 (2007): 178–182.

33. M. Cao, X. Jin, Y. Peng, C. Yu, K. Li, K. Liu, and L. Jiang, "Unidirectional Wetting Properties on Multi-Bioinspired Magnetocontrollable Slippery Microcilia," *Advanced Materials* 29, no. 23 (2017): 1606869.

34. Y. Song, S. Jiang, G. Li, Y. Zhang, H. Wu, C. Xue, H. You, D. Zhang, Y. Cai, and J. Zhu, "Cross-Species Bioinspired Anisotropic Surfaces for Active Droplet Transportation Driven by Unidirectional Microcolumn Waves," *ACS Applied Materials & Interfaces* 12, no. 37 (2020): 42264–42273.

35. C. Zhang, X. Xiao, Y. Zhang, Z. Liu, X. Xiao, A. Nashalian, X. Wang, M. Cao, X. He, and J. Chen, "Bioinspired Anisotropic Slippery Cilia for Stiffness-Controllable Bubble Transport," *ACS Nano* 16, no. 6 (2022): 9348–9358.

36. Y. Wang, H. Lai, Z. Cheng, H. Zhang, E. Zhang, T. Lv, Y. Liu, and L. Jiang, "Gecko Toe Pads Inspired In Situ Switchable Superhydrophobic Shape Memory Adhesive Film," *Nanoscale* 11, no. 18 (2019): 8984–8993.

37. L. Yang, W. Li, J. Lian, H. Zhu, Q. Deng, Y. Zhang, J. Li, X. Yin, and L. Wang, "Selective Directional Liquid Transport on Shoot Surfaces of Crassula Muscosa," *Science* 384, no. 6702 (2024): 1344–1349.

38. X. Liu, M. Gao, B. Li, R. Liu, Z. Chong, Z. Gu, and K. Zhou, *Bioinspired Capillary Transistors. Advanced Materials* 36, no. 41 (2024): 2310797.

39. J. Yang, G. Liu, K. Zhang, P. Li, H. Yan, Y. Yan, Y. Zheng, Z. Zhao, L. Zhang, and X. Liu, "Sunflower-Inspired Superhydrophobic Surface with Composite Structured Microcone Array for Anisotropy Liquid/Ice Manipulation," *Small* 20, no. 52 (2024): 2403420.

40. C. Li, M. Li, Z. Ni, Q. Guan, B. R. Blackman, and E. Saiz, "Stimuli-Responsive Surfaces for Switchable Wettability and Adhesion," *Journal of the Royal Society Interface* 18, no. 179 (2021): 20210162.

41. Y. Li, J. Li, L. Liu, Y. Yan, Q. Zhang, N. Zhang, L. He, Y. Liu, X. Zhang, and D. Tian, "Switchable Wettability and Adhesion of Micro/Nanostructured Elastomer Surface via Electric Field for Dynamic Liquid Droplet Manipulation," *Advanced Science* 7, no. 18 (2020): 2000772.

42. C. Li, F. Cheng, J.-a. Lv, Y. Zhao, M. Liu, L. Jiang, and Y. Yu, "Light-Controlled Quick Switch of Adhesion on a Micro-Arrayed Liquid Crystal Polymer Superhydrophobic Film," *Soft Matter* 8, no. 14 (2012): 3730–3733.

43. K. Okada, Y. Miura, T. Chiya, Y. Tokudome, and M. Takahashi, "Thermo-Responsive Wettability via Surface Roughness Change on Polymer-Coated Titanate Nanorod Brushes toward Fast and Multi-Directional Droplet Transport," *RSC Advances* 10, no. 47 (2020): 28032–28036.

44. M. Wang, D. Chu, L. Liu, S. Huang, X.-M. Chen, Z.-Y. Liu, and H. Yang, "Intelligent Surfaces Thermally Switchable between the Highly rough and Entirely Smooth States," *Chinese Journal of Polymer Science* 39 (2021): 1609–1616.

45. M. Sharma, S. Gupta, B. Bhatt, G. Bhatt, S. Bhattacharya, and K. Khare, "Anisotropic Motion of Aqueous Drops on Lubricated Chemically Heterogenous Slippery Surfaces," *Advanced Materials Interfaces* 8, no. 5 (2021): 2001916.

46. Y. Zhang, Z. Huang, F. Qin, H. Wang, K. Cui, K. Guo, Z. Cai, X. Cai, J. Xiao, and J. Carmeliet, "Connected Three-Dimensional Polyhedral Frames for Programmable Liquid Processing," *Nature Chemical Engineering* 1, no. 7 (2024): 472–482.

47. G. Hou, M. Cao, C. Yu, S. Zheng, D. Wang, Z. Zhu, W. Miao, Y. Tian, and L. Jiang, "Foolproof Method for Fast and Reversible Switching of Water-Droplet Adhesion by Magnetic Gradients," *ACS Applied Materials & Interfaces* 9, no. 27 (2017): 23238–23245.

48. W. Liu, Y. Lu, Y. Shen, H. Chen, Y. Ni, and Y. Xu, "Spontaneous Transport Mechanics of Water Droplets under a Synergistic Action of Designed Pattern and Non-Wetting Gradient," *ACS Omega* 8, no. 18 (2023): 16450–16458, https://doi.org/10.1021/acsomega.3c01536.

49. X. Yang, K. Zhuang, Y. Lu, and X. Wang, "Creation of Topological Ultraslippery Surfaces for Droplet Motion Control," *ACS Nano* 15, no. 2 (2021): 2589–2599, https://doi.org/10.1021/acsnano.0c07417.

50. Q. Rao, Z. Tong, L. Song, A. Ali, Y. Hou, Q. He, J. Lu, X. Gao, X. Zhan, and Q. Zhang, "NIR-Driven Fast Construction of Patterned-Wettability on Slippery Lubricant Infused Surface for Droplet Manipulation," *Chemical Engineering Journal* 428 (2022): 131141.

51. M. Chen, X. Shen, and L. Xu, "Hydrodynamic Metamaterials: Principles, Experiments, and Applications," *Droplet* 2, no. 4 (2023): e79.

52. M. Chen, X. Shen, Z. Chen, J. H. Y. Lo, Y. Liu, X. Xu, Y. Wu, and L. Xu, "Realizing the Multifunctional Metamaterial for Fluid Flow in a Porous Medium," *Proceedings of the National Academy of Sciences* 119, no. 49 (2022): e2207630119.

26884062, 2026, 2, Downloaded from https://onlinelibrary.wiley.com/doi/10.1002/sstr.202500492 by Scholarly Resource Services, Wiley Online Library on [04/11/2026]. See the Terms and Conditions (https://onlinelibrary.wiley.com/terms-and-conditions) on Wiley Online Library for rules of use; OA articles are governed by the applicable Creative Commons License

53. R. David and A. W. Neumann, "Contact Angle Patterns on Low-Energy Surfaces," *Advances in Colloid and Interface Science* 206 (2014), 46–56.

54. W. S. Yang and C.-J. C. Kim, "Structured Surfaces with Engineered Wettability: Fundamentals, Industrial Applications, and Challenges for Commercialization," in Materials with Extreme Wetting Properties: Methods and Emerging Industrial Applications, ed. M. Hosseini and I. Karapanagiotis (Springer, 2021), 63–90.

55. K. Cheng, B. Naccarato, K. J. Kim, and A. Kumar, "Theoretical Consideration of Contact Angle Hysteresis Using Surface-Energy-Minimization Methods," *International Journal of Heat and Mass Transfer* 102 (2016): 154–161.

56. P. Zhu and L. Wang, "Passive and Active Droplet Generation with Microfluidics: A Review," *Lab on a Chip* 17, no. 1 (2017): 34–75.

57. Y. Li, M. Jain, Y. Ma, and K. Nandakumar, "Control of the Breakup Process of Viscous Droplets by an External Electric Field inside a Microfluidic Device," *Soft Matter* 11, no. 19 (2015): 3884–3899.

58. T. Wang, H. Chen, K. Liu, S. Wang, P. Xue, Y. Yu, P. Ge, J. Zhang, and B. Yang, "Janus Si Micropillar Arrays with Thermal-Responsive Anisotropic Wettability for Manipulation of Microfluid Motions," *ACS Applied Materials & Interfaces* 7, no. 1 (2015): 376–382.

59. S.-Z. Wu, J.-N. Wang, L.-G. Niu, J. Yao, D. Wu, and A.-W. Li, "Reversible Switching between Isotropic and Anisotropic Wetting by One-Direction Curvature Tuning on Flexible Superhydrophobic Surfaces," *Applied Physics Letters* 98, no. 8 (2011).

60. J. Seo, S.-K. Lee, J. Lee, J. Seung Lee, H. Kwon, S.-W. Cho, J.-H. Ahn, and T. Lee, "Path-Programmable Water Droplet Manipulations on an Adhesion Controlled Superhydrophobic Surface," *Scientific Reports* 5, no. 1 (2015): 12326.

61. S. Chen, M. Zhu, Y. Zhang, S. Dong, and X. Wang, "Magnetic-Responsive Superhydrophobic Surface of Magnetorheological Elastomers Mimicking From Lotus Leaves to Rose Petals," *Langmuir* 37, no. 7 (2021): 2312–2321.

62. H. Zhou, C. C. Mayorga-Martinez, S. Pané, L. Zhang, and M. Pumera, "Magnetically Driven Micro and Nanorobots," *Chemical Reviews* 121, no. 8 (2021): 4999–5041.

63. Z. Sun and Y. Hou, "Micro/Nanorobots as Active Delivery Systems for Biomedicine: From Self-Propulsion to Controllable Navigation," *Advanced Therapeutics* 5, no. 7 (2022): 2100228.

64. W. Gilpin, M. S. Bull, and M. Prakash, "The Multiscale Physics of Cilia and Flagella," *Nature Reviews Physics* 2, no. 2 (2020): 74–88.

65. V. Sahadevan, B. Panigrahi, and C.-Y. Chen, "Microfluidic Applications of Artificial Cilia: Recent Progress, Demonstration, and Future Perspectives," *Micromachines* 13, no. 5 (2022): 735.

66. S. Zhang, R. Zhang, Y. Wang, P. R. Onck, and J. M. Den Toonder, "Controlled Multidirectional Particle Transportation by Magnetic Artificial Cilia," *ACS Nano* 14, no. 8 (2020): 10313–10323.

67. X. Zhang, J. Guo, X. Fu, D. Zhang, and Y. Zhao, "Tailoring Flexible Arrays for Artificial Cilia Actuators," *Advanced Intelligent Systems* 3, no. 10 (2021): 2000225.

68. S. Ben, T. Zhou, H. Ma, J. Yao, Y. Ning, D. Tian, K. Liu, and L. Jiang, "Multifunctional Magnetocontrollable Superwettable-Microcilia Surface for Directional Droplet Manipulation," *Advanced Science* 6, no. 17 (2019): 1900834.

69. G. Chen, Z. Dai, S. Li, Y. Huang, Y. Xu, J. She, and B. Zhou, "Magnetically Responsive Film Decorated with Microcilia for Robust and Controllable Manipulation of Droplets," *ACS Applied Materials & Interfaces* 13, no. 1 (2021): 1754–1765.

70. C. Yang, L. Wu, and G. Li, "Magnetically Responsive Superhydrophobic Surface: In Situ Reversible Switching of Water Droplet Wettability and Adhesion for Droplet Manipulation," *ACS Applied Materials & Interfaces* 10, no. 23 (2018): 20150–20158.

71. Y. Wang, H. Lai, Z. Cheng, H. Zhang, Y. Liu, and L. Jiang, "Smart Superhydrophobic Shape Memory Adhesive Surface toward Selective Capture/Release of Microdroplets," *ACS Applied Materials & Interfaces* 11, no. 11 (2019): 10988–10997.

72. J. Tan, Z. Fan, M. Zhou, T. Liu, S. Sun, G. Chen, Y. Song, Z. Wang, and D. Jiang, "Orbital Electrowetting-on-Dielectric for Droplet Manipulation on Superhydrophobic Surfaces," *Advanced Materials* 36, no. 24 (2024): 2314346.

73. Y. Zhang, L. Li, G. Li, Z. Lin, R. Wang, D. Chen, Y. Lei, D. Tan, Z. Wang, and Y. Zhao, "Topological Elastic Liquid Diode," *Science Advances* 11, no. 14 (2025): eadt9526.

74. Y. Zhang and N.-T. Nguyen, "Magnetic Digital Microfluidics–a Review," *Lab on a Chip* 17, no. 6 (2017): 994–1008.

75. G. Huang, M. Li, Q. Yang, Y. Li, H. Liu, H. Yang, and F. Xu, "Magnetically Actuated Droplet Manipulation and Its Potential Biomedical Applications," *ACS Applied Materials & Interfaces* 9, no. 2 (2017): 1155–1166.

76. D. Baigl, "Photo-Actuation of Liquids for Light-Driven Microfluidics: State of the Art and Perspectives," *Lab on a Chip* 12, no. 19 (2012): 3637–3653.

77. H. Dai, Z. Dong, and L. Jiang, "Directional Liquid Dynamics of Interfaces with Superwettability," *Science Advances* 6, no. 37 (2020): eabb5528.

78. C. Gao, L. Wang, Y. Lin, J. Li, Y. Liu, X. Li, S. Feng, and Y. Zheng, "Droplets Manipulated on Photothermal Organogel Surfaces," *Advanced Functional Materials* 28, no. 35 (2018): 1803072.

79. S. An, M. Zhu, K. Gu, M. Jiang, Q. Shen, B. Fu, C. Song, P. Tao, T. Deng, and W. Shang, "Light-Driven Motion of Water Droplets with Directional Control on Nanostructured Surfaces," *Nanoscale* 12, no. 7 (2020): 4295–4301.

80. J.-a. Lv, Y. Liu, J. Wei, E. Chen, L. Qin, and Y. Yu, "Photocontrol of Fluid Slugs in Liquid Crystal Polymer Microactuators," *Nature* 537, no. 7619 (2016): 179–184.

81. S.-Y. Park and P.-Y. Chiou, "Light-Driven Droplet Manipulation Technologies for Lab-on-a-Chip Applications," *Advances in OptoElectronics* 2011, no. 1 (2011): 909174.

82. Y. Zhou, S. Huang, and X. Tian, "Magnetoresponsive Surfaces for Manipulation of Nonmagnetic Liquids: Design and Applications," *Advanced Functional Materials* 30, no. 6 (2020): 1906507.

83. Y. Li, L. He, X. Zhang, N. Zhang, and D. Tian, "External-Field-Induced Gradient Wetting for Controllable Liquid Transport: From Movement on the Surface to Penetration into the Surface," *Advanced Materials* 29, no. 45 (2017): 1703802.

84. F. Lapierre, M. Jonsson-Niedziolka, Y. Coffinier, R. Boukherroub, and V. Thomy, "Droplet Transport by Electrowetting: Lets Get rough!," *Microfluidics and Nanofluidics* 15 (2013): 327–336.

85. H. Geng, J. Feng, L. M. Stabryla, and S. K. Cho, "Dielectrowetting Manipulation for Digital Microfluidics: Creating, Transporting, Splitting, and Merging of Droplets," *Lab on a Chip* 17, no. 6 (2017): 1060–1068.

86. F. Mugele and J.-C. Baret, "Electrowetting: From Basics to Applications," *Journal of Physics: Condensed Matter* 17, no. 28 (2005): R705.

87. L. Chen and E. Bonaccurso, Electrowetting—From Statics to Dynamics. *Advances in Colloid and Interface Science* 210, (2014): 2–12.

88. H. H. Vu, N.-T. Nguyen, N.-K. Nguyen, C. H. Luu, S. Hettiarachchi, and N. Kashaninejad, "Tunable Wettability with Stretchable Microstructured Surfaces," *Advanced Engineering Materials* 25, no. 23 (2023): 2300821.

89. J. K. Park and S. Kim, "Droplet Manipulation on a Structured Shape Memory Polymer Surface," *Lab on a Chip* 17, no. 10 (2017): 1793–1801.

26884062, 2026, 2, Downloaded from https://onlinelibrary.wiley.com/doi/10.1002/sstr.202500492 by Scholarly Resource Services, Wiley Online Library on [04/11/2026]. See the Terms and Conditions (https://onlinelibrary.wiley.com/terms-and-conditions) on Wiley Online Library for rules of use; OA articles are governed by the applicable Creative Commons License

90. S. Pisani, I. Genta, T. Modena, R. Dorati, M. Benazzo, and B. Conti, "Shape-Memory Polymers Hallmarks and Their Biomedical Applications in the Form of Nanofibers," *International Journal of Molecular Sciences* 23, no. 3 (2022): 1290.

91. Y. Shao, H. Dou, P. Tao, R. Jiang, Y. Fan, Y. Jiang, J. Zhao, Z. Zhang, T. Yue, and S. N. Gorb, "Precise Controlling of Friction and Adhesion on Reprogrammable Shape Memory Micropillars," *ACS Applied Materials & Interfaces* 14, no. 15 (2022): 17995–18003.

92. Y. Chen, C. Chen, H. U. Rehman, X. Zheng, H. Li, H. Liu, and M. S. Hedenqvist, "Shape-Memory Polymeric Artificial Muscles: Mechanisms, Applications and Challenges," *Molecules (Basel, Switzerland)* 25, no. 18 (2020): 4246.

93. L. Santo, F. Quadrini, D. Bellisario, and L. Iorio, "Applications of Shape-Memory Polymers, and Their Blends and Composites," in Shape Memory Polymers, Blends and Composites: Advances and Applications (Springer Singapore, 2019), 311–329.

94. M. Tenjimbayashi and K. Manabe, "A Review on Control of Droplet Motion Based on Wettability Modulation: Principles, Design Strategies, Recent Progress, and Applications," *Science and Technology of Advanced Materials* 23, no. 1 (2022): 473–497.

95. K. Funayama, A. Miura, and H. Tanaka, "Flexibly Designable Wettability Gradient for Passive Control of Fluid Motion via Physical Surface Modification," *Scientific Reports* 13, no. 1 (2023): 6440.

96. A. Mehran, P. Rostami, M. S. Saidi, B. Firoozabadi, and N. High-Throughput Kashaninejad, "Label-Free Isolation of White Blood Cells From Whole Blood Using Parallel Spiral Microchannels with U-Shaped Cross-Section," *Biosensors* 11, no. 11 (2021): 406.

97. B. Chang, Q. Zhou, R. H. Ras, A. Shah, Z. Wu, and K. Hjort, "Sliding Droplets on Hydrophilic/Superhydrophobic Patterned Surfaces for Liquid Deposition," *Applied Physics Letters* 108, no. 15 (2016).

98. T. Dimitriadis, L. Stendardo, I. Tagliaro, A. M. Coclite, C. Antonini, and T. Maitra, "Capillary-Driven Water Transport by Contrast Wettability-Based Durable Surfaces," *ACS Applied Materials & Interfaces* 15, no. 22 (2023): 27206–27213.

99. H. Zhang, Y. Liu, Z. Zhang, M. Hua, and G. Dong, "A Superhydrophobic Surface Patterned with Hydrophilic Channels for Directional Sliding Control and Manipulation of Droplets," *Surface and Coatings Technology* 409 (2021): 126836.

100. J. Liu, H. Guo, B. Zhang, S. Qiao, M. Shao, X. Zhang, X. Q. Feng, Q. Li, Y. Song, and L. Jiang, "Guided Self-Propelled Leaping of Droplets on a Micro-Anisotropic Superhydrophobic Surface," *Angewandte Chemie International Edition* 55, no. 13 (2016): 4265–4269.

101. J. E. Mates, T. M. Schutzius, J. Qin, D. E. Waldroup, and C. M. Megaridis, "The Fluid Diode: Tunable Unidirectional Flow through Porous Substrates," *ACS Applied Materials & Interfaces* 6, no. 15 (2014): 12837–12843.

102. J. Li, X. Zhou, J. Li, L. Che, J. Yao, G. McHale, M. K. Chaudhury, and Z. Wang, *Topological Liquid Diode. Science Advances* 3, no. 10 (2017): eaao3530.

103. J. Wang, B. Cui, H. Liu, X. Chen, Y. Li, R. Wang, T. Lang, H. Yang, l. Li, and H. Pan, "Tesla Valve-Based Flexible Microhybrid Chip with Unidirectional Flow Properties," *ACS Omega* 7, no. 36 (2022): 31744–31755.

104. C. Yang, W. Li, Y. Zhao, and L. Shang, "Flexible Liquid-Diode Microtubes From Multimodal Microfluidics," *Proceedings of the National Academy of Sciences* 121, no. 28 (2024): e2402331121.

105. J. Li, Y. Song, H. Zheng, S. Feng, W. Xu, and Z. Wang, *Designing Biomimetic Liquid Diodes. Soft Matter* 15, no. 9 (2019): 1902–1915.

106. T. Zhang, M. Li, B. Su, C. Ye, K. Li, W. Shen, L. Chen, Z. Xue, S. Wang, and L. Jiang, "Bio-Inspired Anisotropic Micro/Nano-Surface From a Natural Stamp: Grasshopper Wings," *Soft Matter* 7, no. 18 (2011): 7973–7975.

107. Q. Li, L. Li, K. Shi, B. Yang, X. Wang, Z. Shi, D. Tan, F. Meng, Q. Liu, and S. Hu, "Reversible Structure Engineering of Bioinspired Anisotropic Surface for Droplet Recognition and Transportation," *Advanced Science* 7, no. 18 (2020): 2001650.

108. C. Y. Huang, M. F. Lai, W. L. Liu, and Z. H. Wei, "*Anisotropic Wettability of Biomimetic Micro/Nano Dual-Scale Inclined Cones Fabricated by Ferrofluid-Molding Method." Advanced Functional Materials*, 25, no. 18 (2015): 2670–2676.

109. B. Guo, J. Sun, Y. Hua, N. Zhan, J. Jia, and K. Chu, "Femtosecond Laser Micro/Nano-Manufacturing: Theories, Measurements, Methods, and Applications," *Nanomanufacturing and Metrology* 3 (2020): 26–67.

110. A. Volpe, U. Krishnan, M. S. Chiriacò, E. Primiceri, A. Ancona, and F. Ferrara, "A Smart Procedure for the Femtosecond Laser-Based Fabrication of a Polymeric Lab-on-a-Chip for Capturing Tumor Cell," *Engineering* 7, no. 10 (2021): 1434–1440.

111. G. Schnell, C. Jagow, A. Springer, M. Frank, and H. Seitz, "Time-Dependent Anisotropic Wetting Behavior of Deterministic Structures of Different Strut Widths on Ti6Al4V," *Metals* 9, no. 9 (2019): 938.

112. H. Zhang, P. Wang, Y. Liu, S. Dai, Y. Zhu, B. Li, and G. Dong, "Stretch-Controlled Branch Shape Microstructures for Switchable Unidirectional Self-Driven Spreading of Oil Droplets," *ACS Applied Materials & Interfaces* 16, no. 31 (2024): 41694–41703.

113. S. Lakshminarayanan, "Micro/Nano Patterning on Polymers Using Soft Lithography Technique," *Micro/Nanolithography-A Heuristic Aspect on the Enduring Technology* (2018), https://doi.org/10.5772/intechopen.72885.

114. N. P. U. Mai and P.-Y. Chen, "Investigation on the Anisotropic Wetting Properties of Water Droplets on Bio-Inspired Groove Structures Fabricated by 3D Printing and Surface Modifications," *Biomimetics* 7, no. 4 (2022): 174.

115. Y. Wang, C. Gao, W. Zhao, G. Zheng, Y. Ji, K. Dai, L. Mi, D. Zhang, C. Liu, and C. Shen, "Large-Area Fabrication and Applications of Patterned Surface with Anisotropic Superhydrophobicity," *Applied Surface Science* 529 (2020): 147027.

116. L. Jiao, D. Tan, Y. Hu, Y. Yang, Q. Guo, N. Zhou, H. Wu, C. Chen, X. Zhao, and G. Hu, "Efficient Fabrication of Bioinspired Soft, Ridged-Slippery Surfaces with Large-Range Anisotropic Wettability for Droplet Manipulation," *Soft Matter* 20, no. 12 (2024): 2812–2822.

117. A. Al-Azawi, C. Hörenz, T. Tupasela, O. Ikkala, V. Jokinen, S. Franssila, and R. H. Ras, "Slippery and Magnetically Responsive Micropillared Surfaces for Manipulation of Droplets and Beads," *AIP Advances* 10 (2020): 8.

118. A. F. Demirörs, S. Aykut, S. Ganzeboom, Y. A. Meier, and E. Poloni, "Programmable Droplet Manipulation and Wetting with Soft Magnetic Carpets," *Proceedings of the National Academy of Sciences* 118, no. 46 (2021): e2111291118.

119. J. Wang, Z. Zhu, P. Liu, S. Yi, L. Peng, Z. Yang, X. Tian, and L. Jiang, "Magneto-Responsive Shutter for on-Demand Droplet Manipulation," *Advanced Science* 8, no. 23 (2021): 2103182.

120. Q. Zhang, L. He, X. Zhang, D. Tian, and L. Jiang, "Switchable Direction of Liquid Transport via an Anisotropic Microarray Surface and Thermal Stimuli," *ACS Nano* 14, no. 2 (2020): 1436–1444.

121. X. Liang and Z. Guo, "Mechano-Adjusted Anisotropic Surface for Manipulating Water Droplets," *Chemical Engineering Journal* 395 (2020): 125110.

122. X. Bai, Q. Yang, Y. Fang, J. Yong, Y. Bai, J. Zhang, X. Hou, and F. Chen, "Anisotropic, Adhesion-Switchable, and Thermal-Responsive Superhydrophobicity on the Femtosecond Laser-Structured Shape-Memory Polymer for Droplet Manipulation," *Chemical Engineering Journal* 400 (2020): 125930.

123. W.-Q. Ye, Y.-Y. Wei, D.-N. Wang, C.-G. Yang, and Z.-R. Xu, "A Digital Microfluidic Platform Based on a Near-Infrared Light-

26884062, 2026, 2, Downloaded from https://onlinelibrary.wiley.com/doi/10.1002/sstr.202500492 by Scholarly Resource Services, Wiley Online Library on [04/11/2026]. See the Terms and Conditions (https://onlinelibrary.wiley.com/terms-and-conditions) on Wiley Online Library for rules of use; OA articles are governed by the applicable Creative Commons License

Responsive Shape-Memory Micropillar Array," *Lab on a Chip* 21, no. 6 (2021): 1131–1138.

124. X. Yang, Y. Li, H. Zheng, and Y. Lu, "Saturated Surface Charging on Micro/Nanoporous Polytetrafluoroethylene for Droplet Manipulation," *ACS Applied Nano Materials* 5, no. 3 (2022): 3342–3351.

125. H. Wu, K. Zhu, B. Cao, Z. Zhang, B. Wu, L. Liang, G. Chai, and A. Liu, "Smart Design of Wettability-Patterned Gradients on Substrate-Independent Coated Surfaces to Control Unidirectional Spreading of Droplets," *Soft Matter* 13, no. 16 (2017): 2995–3002.

126. Y. Nakashima, Y. Nakanishi, and T. Yasuda, "Automatic Droplet Transportation on a Plastic Microfluidic Device Having Wettability Gradient Surface," *Review of Scientific Instruments* 86, no. 1 (2015): 015001.

127. C. Liu, J. Sun, J. Li, C. Xiang, L. Che, Z. Wang, and X. Zhou, "Long-Range Spontaneous Droplet Self-Propulsion on Wettability Gradient Surfaces," *Scientific Reports* 7, no. 1 (2017): 7552.

128. Z. Yu, F. F. Yun, Y. Wang, L. Yao, S. Dou, K. Liu, L. Jiang, and X. Wang, "Desert Beetle-Inspired Superwettable Patterned Surfaces for Water Harvesting," *Small (weinheim an Der Bergstrasse, Germany)* 13, no. 36 (2017): 1701403.

129. J. Wu, K. Yin, S. Xiao, Z. Wu, Z. Zhu, J. A. Duan, and J. He, "Laser Fabrication of Bioinspired Gradient Surfaces for Wettability Applications," *Advanced Materials Interfaces* 8, no. 5 (2021): 2001610.

130. X. Yang, X. Liu, Y. Lu, J. Song, S. Huang, S. Zhou, Z. Jin, and W. Xu, "Controllable Water Adhesion and Anisotropic Sliding on Patterned Superhydrophobic Surface for Droplet Manipulation," *The Journal of Physical Chemistry C* 120, no. 13 (2016): 7233–7240.

131. M. Zhang, L. Wang, Y. Hou, W. Shi, S. Feng, and Y. Zheng, "Controlled Smart Anisotropic Unidirectional Spreading of Droplet on a Fibrous Surface," *Advanced Materials* 27, no. 34 (2015): 5057–5062.

132. E. L. Zoudani, N.-T. Nguyen, and N. Kashaninejad, "Surface Engineering for Enhanced Wicking: The Role of Laser Machining and Surface Roughness," *Journal of Science: Advanced Materials and Devices* 9, no. 4 (2024): 100819.

133. J. Lee, S. Hwang, D.-H. Cho, J. Hong, J. H. Shin, and D. Byun, "RF Plasma Based Selective Modification of Hydrophilic Regions on Super Hydrophobic Surface," *Applied Surface Science* 394 (2017): 543–553.

134. H. Liu, L. Zhang, J. Huang, X. Zhang, J. Mao, Z. Chen, Q. Mao, M. Ge, and Y. Lai, "Superwetting Patterned PDMS/PMMA Materials by Facile One-Step Electro-Spraying for Signal Expression and Liquid Transportation," *Chemical Engineering Journal* 431 (2022): 133206.

135. D. Li, Y. Fan, G. Han, and Z. Guo, "Multibioinspired Janus Membranes with Superwettable Performance for Unidirectional Transportation and Fog Collection," *Chemical Engineering Journal* 404 (2021): 126515.

136. Y.-y. Song, Z.-p. Yu, L.-m. Dong, M.-l. Zhu, Z.-c. Ye, Y.-j. Shi, and Y. Liu, "Cactus-Inspired Janus Membrane with a Conical Array of Wettability Gradient for Efficient Fog Collection," *Langmuir : the Acs Journal of Surfaces and Colloids* 37, no. 46 (2021): 13703–13711.

137. E. Bazigou and T. Makinen, "Flow Control in Our Vessels: Vascular Valves Make Sure There Is No Way Back," *Cellular and Molecular Life Sciences : Cmls* 70, no. 6 (2013): 1055–1066, https://doi.org/10.1007/s00018-012-1110-6.

138. J. W. Noordzij and N. F. Dabhoiwala, "A View on the Anatomy of the Ureterovesical Junction," *Scandinavian Journal of Urology and Nephrology* 27, no. 3 (1993): 371–380, https://doi.org/10.3109/00365599309180449.

139. T. Cserni, S. Paran, Z. Kanyari, A. M. O'Donnell, B. Kutasy, N. Nemeth, and P. Puri, "New Insights into the Neuromuscular Anatomy of the Ileocecal Valve." *Anatamical Record (Hoboken)* 292, no. 2 (2009): 254–261, https://doi.org/10.1002/ar.20839.

140. S. C. Leigh, A. P. Summers, S. L. Hoffmann, and D. P. German, "Shark Spiral Intestines May Operate as Tesla Valves," *Proceedings. Biological Sciences* 288, no. 1955 (2021): 20211359, https://doi.org/10.1098/rspb.2021.1359.

141. A. Bas-Cristobal Menendez, Z. Du, T. P. P. van den Bosch, A. Othman, N. Gaio, C. Silvestri, W. Quiros, H. Lin, S. Korevaar, A. Merino, J. Mulder, and M. J. Hoogduijn, "Creating a Kidney Organoid-Vasculature Interaction Model Using a Novel Organ-on-Chip System," *Scientific Reports* 12, no. 1 (2022): 20699, https://doi.org/10.1038/s41598-022-24945-5.

142. Y. I. Wang and M. L. Shuler, "UniChip Enables Long-Term Recirculating Unidirectional Perfusion with Gravity-Driven Flow for Microphysiological Systems," *Lab on A Chip* 18, no. 17 (2018): 2563–2574, https://doi.org/10.1039/c8lc00394g.

143. M. Busek, A. Aizenshtadt, T. Koch, A. Frank, L. Delon, M. A. Martinez, A. Golovin, C. Dumas, J. Stokowiec, S. Gruenzner, E. Melum, and S. Krauss, "Pump-less, Recirculating Organ-on-a-Chip (rOoC) Platform," *Lab Chip* 23, no. 4 (2023): 591–608, https://doi.org/10.1039/d2lc00919f.

144. J. Feng and J. P. Rothstein, "One-Way Wicking in Open Micro-Channels Controlled by Channel Topography," *Journal of Colloid and Interface Science* 404 (2013): 169–178, https://doi.org/10.1016/j.jcis.2013.02.052.

145. A. Purwidyantri and B. A. Prabowo, "*Tesla Valve Microfluidics: The Rise of Forgotten Technology. Chemosensors*" 11, no. 4 (2023), https://doi.org/10.3390/chemosensors11040256.

146. D. Chen, J. Chen, M. Wu, H. Tian, X. Chen, and J. Sun, "Robust and Flexible Free-Standing Films for Unidirectional Drug Delivery," *Langmuir : the Acs Journal of Surfaces and Colloids* 29, no. 26 (2013): 8328–8334, https://doi.org/10.1021/la401423d.

147. K. Huang, Y. Si, and J. Hu, "Fluid Unidirectional Transport Induced by Structure and Ambient Elements across Porous Materials: From Principles to Applications," *Advanced Materials* 36, no. 32 (2024): e2402527, https://doi.org/10.1002/adma.202402527.

148. W. Zhou, S. Min, T. Zhan, Y. Zhang, D. Pan, Y. Yuan, and B. Xu, "Highly Durable Janus Fabrics Based on Transfer Prints for Personal Moisture Management," *Small (weinheim an Der Bergstrasse, Germany)* 19, no. 36 (2023): e2302512, https://doi.org/10.1002/smll.202302512.

149. Y. Wang, X. Liang, H. Zhu, J. H. Xin, Q. Zhang, and S. Zhu, "*Reversible Water Transportation Diode: Temperature-Adaptive Smart Janus Textile for Moisture/Thermal Management." Advanced Functional Materials*30, no. 6 (2020), https://doi.org/10.1002/adfm.201907851.

150. B. Dai, K. Li, L. Shi, X. Wan, X. Liu, F. Zhang, L. Jiang, and S. Wang, "Bioinspired Janus Textile with Conical Micropores for Human Body Moisture and Thermal Management," *Advanced Materials* 31, no. 41 (2019): e1904113, https://doi.org/10.1002/adma.201904113.

151. J. Dong, Y. Peng, X. Nie, L. Li, C. Zhang, F. Lai, G. He, P. Ma, Q. Wei, Y. Huang, and T. Liu, "Hierarchically Designed Super-Elastic Metafabric for Thermal-Wet Comfortable and Antibacterial Epidermal Electrode," *Advanced Functional Materials* 32 (2022): 48, https://doi.org/10.1002/adfm.202209762.

152. H. Wu, B. Gao, H. Wu, J. Song, L. Zhu, M. Zhou, X. Linghu, S. Huang, Z. Zhou, and Q. Wa, "A Unidirectional Water-Transport Antibacterial Bilayer Nanofibrous Dressing Based on Chitosan for Accelerating Wound Healing," *International Journal of Biological Macromolecules* 269, no. 269 (Pt 2) (2024): 131878, https://doi.org/10.1016/j.ijbiomac.2024.131878.

153. K. Guo, K. Ou, M. A. Amin Newton, J. Zhang, H. Xu, J. Li, B. Xin, and Y. Huang, "Multifunctional Janus Nanofibrous Membrane with Unidirectional Water Transport and pH-Responsive Color-Changing for Wound Dressing," *Journal of Colloid and Interface Science* 679 (Pt B) (2025): 723–736, https://doi.org/10.1016/j.jcis.2024.10.137.

26884062, 2026, 2, Downloaded from https://onlinelibrary.wiley.com/doi/10.1002/sstr.202500492 by Scholarly Resource Services, Wiley Online Library on [04/11/2026]. See the Terms and Conditions (https://onlinelibrary.wiley.com/terms-and-conditions) on Wiley Online Library for rules of use; OA articles are governed by the applicable Creative Commons License

154. H. Pi, Y. Xi, J. Wu, M. Hu, B. Tian, Y. Yang, R. Wang, and X. Zhang, "Janus Fibrous Membrane with Directional Liquid Transport Capacity for Wound Healing Promotion," *Chemical Engineering Journal* 455 (2023), https://doi.org/10.1016/j.cej.2022.140853.

155. S. Cheng, W. Hao, Y. Wang, Y. Wang, and S. Yang, "Commercial Janus Fabrics as Reusable Facemask Materials: A Balance of Water Repellency, Filtration Efficiency, Breathability, and Reusability," *ACS Applied Materials & Interfaces* 14, no. 28 (2022): 32579–32589, https://doi.org/10.1021/acsami.2c09544.

156. X.-Y. Guo, L. Zhao, H.-N. Li, H.-C. Yang, J. Wu, H.-Q. Liang, C. Zhang, and Z.-K. Xu, "Janus Channel of Membranes Enables Concurrent Oil and Water Recovery From Emulsions," *Science* 386, no. 6722 (2024): 654–659.

157. Z. Wang, Y. Shao, T. Wang, J. Zhang, Z. Cui, J. Guo, S. Li, and Y. Chen, "Janus Membranes with Asymmetric Superwettability for High-Performance and Long-Term On-Demand Oil/Water Emulsion Separation," *ACS Applied Materials & Interfaces* 16, no. 12 (2024): 15558–15568, https://doi.org/10.1021/acsami.4c00007.

158. M. Li, K. J. Lu, L. Wang, X. Zhang, and T.-S. Chung, "Janus Membranes with Asymmetric Wettability via a Layer-by-Layer Coating Strategy for Robust Membrane Distillation," *Journal of Membrane Science* 603 (2020), https://doi.org/10.1016/j.memsci.2020.118031.

159. S. Sun, Y. Wang, B. Sun, F. Zhang, Q. Xu, H. Y. Mi, H. Li, X. Tao, Z. Guo, C. Liu, and C. Shen, "Versatile Janus Composite Nonwoven Solar Absorbers with Salt Resistance for Efficient Wastewater Purification and Desalination," *ACS Applied Materials & Interfaces* 13, no. 21 (2021): 24945–24956, https://doi.org/10.1021/acsami.1c05618.

160. J. Lei and Z. Guo, "A Fog-Collecting Surface Mimicking the Namib Beetle: Its Water Collection Efficiency and Influencing Factors," *Nanoscale* 12, no. 13 (2020): 6921–6936, https://doi.org/10.1039/c9nr10808d.

161. Y. Yang, Z. Dai, Y. Chen, and F. Xu, "Active Twisting for Adaptive Droplet Collection," *Nature Computational Science* 5, (2025): 313–321, https://doi.org/10.1038/s43588-025-00786-w.

162. L. Wang, K. Yin, Q. Deng, Q. Huang, J. He, and J. A. Duan, "Wetting Ridge-Guided Directional Water Self-Transport," *Advanced Science* 9, no. 34 (2022): 2204891.

163. B. Dean and B. Bhushan, "Shark-Skin Surfaces for Fluid-Drag Reduction in Turbulent Flow: A Review," *Philosophical Transactions. Series A, Mathematical, Physical, and Engineering Sciences* 368, no. 1929 (2010): 4775–4806, https://doi.org/10.1098/rsta.2010.0201.

164. D. Chen, Y. Liu, H. Chen, and D. Zhang, "Bio-Inspired Drag Reduction Surface From Sharkskin," *Biosurface and Biotribology* 4, no. 2 (2018): 39–45, https://doi.org/10.1049/bsbt.2018.0006.

165. D. Tanaka, D. Buenger, H. Hildebrandt, M. Moeller, and J. Groll, "Unidirectional Control of Anisotropic Wetting through Surface Modification of PDMS Microstructures," *Langmuir* 29, no. 40 (2013): 12331–12336.

166. J. Hu, Y. Peng, Y. Bian, K. Shao, Z. Cui, Y. Zhang, Y. Hu, J. Li, D. Wu, and Y. Zhang, "Geometry-Gradient Magnetocontrollable Lubricant-Infused Microwall Array for Passive/Active Hybrid Bidirectional Droplet Transport," *Langmuir* 39, no. 27 (2023): 9358–9366.

167. L. He, W. Liang, Z. Wang, and A. Akbarzadeh, A Three-Dimensional Model for Analyzing the Anisotropic Wetting Behavior of Striped Surfaces. *Colloids and Surfaces A: Physicochemical and Engineering Aspects* 552, (2018): 67–74.

168. B. Jiang, G. Pan, C. Zheng, X.-H. Wang, Y. Zhang, J. Yin, and H. Zhu, "Dynamic Characteristics and Energy Variation of Droplet Impacting on a Quartz Surface," *Physics of Fluids* 37, no. 2 (2025), https://doi.org/10.1063/5.0251456.

Biographies



Elham Lori Zoudani received both her bachelor's and master's degrees in mechanical engineering from Shahid Chamran University (SCU) and Khaje Nasir Toosi University of Technology (KNTU), Iran, in 2015 and 2019, respectively. In 2023, she joined the Queensland Micro- and Nanotechnology Centre (QMNC), now called the Quantum and Advanced Technologies Research Institute (QUATRI), at Griffith University, Australia, as a PhD candidate. Her research focuses on microneedle design and development for biomedical applications. Her research interests are microfluidics, biomedical microdevices, and computational fluid dynamics.



Nam-Trung Nguyen received his Dip-Ing, Dr Ing, and Dr Ing Habil degrees from Chemnitz University of Technology, Germany, in 1993, 1997, and 2004, respectively. From 1999 to 2013, he was an associate professor at Nanyang Technological University, Singapore. From 2013 to 2023, he was a professor and director of the Queensland Micro- and Nanotechnology Centre at Griffith University, Australia. In 2023, he was awarded the prestigious Australian Laureate Fellowship for advancing the field of microfluidics. He is a fellow of ASME and a senior member of IEEE. He is also an elected fellow of the American Society of Mechanical Engineers.



Navid Kashaninejad received his PhD from Nanyang Technological University (NTU), Singapore. He has extensive expertise in the design and fabrication of microfluidic devices for biomedical and sensing applications. In 2021, he was awarded the prestigious ARC DECRA Fellowship in recognition of his outstanding contributions to the field. Dr. Kashaninejad is currently pioneering the emerging discipline of surface microfluidics and has founded the SUMMIT (Surface Microfluidics, Mechanobiology, and Innovative Technologies) Lab at Griffith University. His research focuses on advanced fabrication techniques and the physics of complex surface interactions, driving innovations that span from next-generation microfluidic platforms to cutting-edge biosensing technologies.

26884062, 2026, 2, Downloaded from https://onlinelibrary.wiley.com/doi/10.1002/sstr.202500492 by Scholarly Resource Services, Wiley Online Library on [04/11/2026]. See the Terms and Conditions (https://onlinelibrary.wiley.com/terms-and-conditions) on Wiley Online Library for rules of use; OA articles are governed by the applicable Creative Commons License